ORIGINAL ARTICLE

Urinary beta-2 microglobulin and alpha-1 microglobulin are useful screening markers for tenofovir-induced kidney tubulopathy in patients with HIV-1 infection: a diagnostic accuracy study

Takeshi Nishijima · Takuro Shimbo · Hirokazu Komatsu ·
Misao Takano · Junko Tanuma · Kunihisa Tsukada · Katsuji Teruya ·
Hiroyuki Gatanaga · Yoshimi Kikuchi · Shinichi Oka

Abstract Kidney tubulopathy is a well-known adverse event of antiretroviral agent tenofovir. A cross-sectional study was conducted to compare the diagnostic accuracy of five tubular markers, with a collection of abnormalities in these markers as the reference standard. The study subjects were patients with HIV-1 infection on ritonavir-boosted darunavir plus tenofovir/emtricitabine with suppressed viral load. Kidney tubular dysfunction (KTD) was predefined as the presence of at least three abnormalities in the following five parameters: β2-microglobulinuria (β2M), α1-microglobulinuria (α1M), high urinary N-acetyl-β-D-glucosaminidase (NAG), fractional excretion of phosphate (FE_{IP}), and fractional excretion of uric acid (FE_{UA}). Receiver operating characteristic curves and areas under the curves (AUC) were estimated, and the differences between the largest AUC and each of the other AUCs were tested using a nonparametric method. The cutoff value of each tubular marker was determined using raw data of 100 % sensitivity with maximal specificity. KTD was diagnosed in 19 of the 190 (10 %) patients. The AUCs (95 % CIs) of each tubular marker were β2M, 0.970 (0.947–0.992); α1M, 0.968 (0.944–0.992); NAG, 0.901 (0.828–0.974); FE_{IP}, 0.757 (0.607–0.907), and FE_{UA}, 0.762 (0.653–0.872). The AUCs of β2M and α1M were not significantly different, whereas those of the other three markers were smaller. The optimal cutoff values with 100 % sensitivity were 1,123 μg/gCr (β2M, specificity 89 %), 15.4 mg/gCr (α1M, specificity 87 %), 3.58 U/gCr (NAG, specificity 46 %), 1.02 % (FE_{IP}, specificity 0 %), and 3.92 % (FE_{UA}, specificity 12 %). Urinary β2M and α1M are potentially suitable screening tools for tenofovir-induced KTD. Monitoring either urinary β2M or α1M should be useful in early detection of tenofovir nephrotoxicity.

Keywords Tenofovir · Kidney tubular dysfunction · Screening · Urinary beta-2 microglobulin · Urinary alpha-1 microglobulin · HIV-1 infection

T. Nishijima · M. Takano · J. Tanuma · K. Tsukada ·
K. Teruya · H. Gatanaga (✉) · Y. Kikuchi · S. Oka
AIDS Clinical Center, National Center for Global Health
and Medicine, 1-21-1, Toyama, Shinjuku,
Tokyo 162-0052, Japan
e-mail: higatana@acc.ncgm.go.jp

T. Nishijima · H. Gatanaga · S. Oka
Center for AIDS Research, Kumamoto University,
Kumamoto, Japan

T. Shimbo
Department of Clinical Research and Informatics, International
Clinical Research Center, National Center for Global Health
and Medicine, 1-21-1, Toyama, Shinjuku, Tokyo, Japan

H. Komatsu
Department of Community Care, Saku Central Hospital,
Nagano, Japan

Introduction

Tenofovir disoproxil fumarate (TDF), a prodrug of tenofovir, is a widely used nucleotide reverse transcriptase inhibitor (NRTI) as part of the initial antiretroviral therapy for patients with human immunodeficiency (HIV) infection, as well as in treatment of hepatitis B virus infection [1–4]. Tenofovir is excreted through the kidney by glomerular filtration and active tubular secretion. Renal proximal tubular damage is a well-known adverse effect of tenofovir, which sometimes leads to diabetes insipidus, Fanconi syndrome, and acute renal failure [5–7], and patients on TDF are more likely to develop renal dysfunction than those on other NRTIs [8, 9]. Of note, low

bone mineral density, another adverse effect of TDF, sometimes occurs as a result of kidney proximal tubulopathy associated with phosphate wasting and increased bone turnover [10, 11].

The risk of clinically relevant tenofovir-induced nephrotoxicity is considered to be relatively low [9, 12, 13]. However, tenofovir renal safety has not been confirmed in the long term. Importantly, both HIV infection and hepatitis B infection require long-term treatment, especially for HIV infection, where the treatment is lifelong. In tenofovir-induced nephrotoxicity, tubular dysfunction usually precedes the decline in glomerular filtration rate (GFR), suggesting that tubular markers are more sensitive than estimated GFR (eGFR) calculated with serum creatinine in screening for tenofovir nephrotoxicity [9, 14–16]. Thus, it is important to identify a renal tubular marker with high sensitivity to screen for tenofovir-induced KTD.

There is no gold standard for the diagnosis of tenofovir-induced kidney tubular dysfunction (KTD). Previous reports usually applied a collection of abnormalities in tubular function parameters as diagnostic criteria [17, 18]. However, the criteria used in each study differ, and it is often cumbersome and costly to monitor multiple renal tubular markers in practice. To our knowledge, there are no studies that have compared the diagnostic accuracy of various tubular markers for tenofovir-induced KTD. Furthermore, several pathological conditions are associated with KTD, such as active infection, diabetic nephropathy, and preexisting renal impairment [19, 20], making it difficult to evaluate KTD induced exclusively by tenofovir.

Based on the foregoing background, we designed the present study to identify the best screening marker(s) of tubular dysfunction in tenofovir-induced KTD, using a collection of abnormalities in kidney tubular markers as the reference standard.

Patients and methods

Ethics statement

This study was approved by the Human Research Ethics Committee of the National Center for Global Health and Medicine, Tokyo, Japan. Each patient in this study provided a written informed consent for publication of clinical data for research purpose. The study was conducted according to the principles expressed in the Declaration of Helsinki.

Study design

This study was designed and reported according to the recommendations of the standards for reporting of diagnostic accuracy (STARD) statement [21]. We performed a single-center cross-sectional study to compare the diagnostic accuracies of various kidney tubular markers for tenofovir-induced KTD, with a collection of abnormalities in these markers as the reference standard, to identify the best screening marker in tenofovir-treated Japanese patients with HIV infection.

Study subjects

The study population has been previously reported [22]. The study enrolled consecutive Japanese patients with HIV infection, aged >17 years, with HIV-1 viral load <200 copies/ml, and on at least 4-week treatment with once-daily ritonavir (100 mg)-boosted darunavir (800 mg) plus fixed-dose tenofovir (300 mg)/emtricitabine (200 mg), seen at our clinic between October 1, 2011 and March 31, 2012. The exclusion criteria were (1) active infection, (2) malignancy, (3) diabetes mellitus, defined by the use of glucose-lowering agents or fasting plasma glucose >126 mg/dl or plasma glucose >200 mg/dl on two different days, (4) alanine aminotransferase 2.5 times more than the upper limit of normal, (5) estimated glomerular filtration rate (eGFR) calculated by Cockcroft–Gault equation of <50 ml/min [creatinine clearance = [(140 − age) × weight (kg)]/ (serum creatinine × 72)(×0.85 for females)] [23], and (6) patients who did not sign the consent form.

Measurements

Blood and spot urine samples were collected on the same day (either on the day of enrollment or on the next visit), together with body weight measurement. The blood samples were used to measure serum creatinine, serum uric acid, serum phosphate, CD4 count, and C-reactive protein (CRP); urine samples were used to measure phosphate, uric acid, creatinine, β2-microglobulin (β2M), α1-microglobulin (α1M), and N-acetyl-β-D-glucosaminidase (NAG). The values of β2M, α1M, and NAG measured in the urine samples were expressed relative to urinary creatinine of 1 gl/l (/g Cr) [24].

Urinary concentrations of β2M and α1M were measured with a latex aggregation assay kit (β2M, BMG-Latex X1 "Seiken"; Denka Seiken, Niigata, Japan; α1M, Eiken α1M-III; Eiken Chemical, Tokyo, Japan), and those of NAG by colorimetric assay of enzyme activity with 6-methyl-2-pyridyl-N-acetyl-1-thio-β-D-glucosaminide as substrate (Nittobo Medical, Tokyo, Japan).

Definition of renal proximal tubular dysfunction

KTD was predefined as the presence of at least three abnormalities in the following five parameters: fractional excretion of phosphate (FE_{IP}) {[(urine phosphate × serum creatinine)/ (serum phosphate × urine creatinine)] × 100} > 18 %,

fractional excretion of uric acid (FE$_{UA}$) {[(urine uric acid × serum creatinine)/(serum uric acid × urine creatinine)] × 100)} > 15 %, β2-microglobulinuria (β2M > 1,000 μg/g Cr), α1-microglobulinuria (α1M > 16.6 mg/g Cr), and high NAG level in urine (NAG > 5.93 U/g Cr). The definition of KTD and the foregoing cutoff levels were determined based on the published reports [18, 25, 26].

The potential risk factors for KTD were determined according to previous studies and collected together with the basic demographics from the medical records [14, 27–30]: included were age, sex, body weight, and presence or absence of other medical conditions (concurrent use of other nephrotoxic drugs such as ganciclovir, sulfamethoxazole/trimethoprim, and nonsteroidal antiinflammatory agents; coinfection with hepatitis B, defined by positive hepatitis B surface antigen; coinfection with hepatitis C, defined by positive HCV viral load; hypertension, defined by current treatment with antihypertensive agents or two successive measurements of systolic blood pressure >140 mmHg or diastolic blood pressure >90 mmHg in the clinic; dyslipidemia, defined by current treatment with lipid-lowering agents or two successive measurements of either low density lipoprotein cholesterol >140 mg/dl, high density lipoprotein cholesterol <40 mg/dl, total cholesterol >240 mg/dl, triglyceride >500 mg/dl). At our clinic, blood pressure and body weight are measured every visit. We used the data on or closest to and preceding the day of blood/urine sample collection by no more than 180 days.
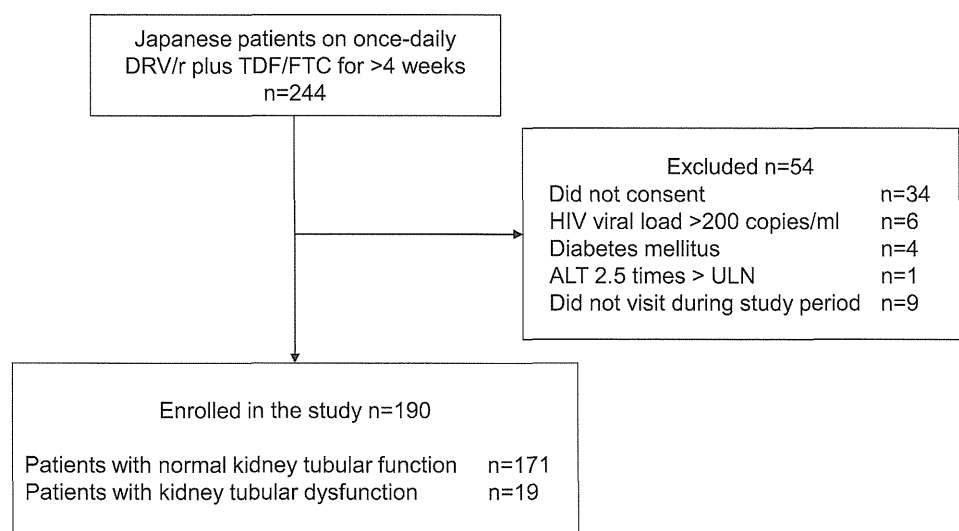
Statistical analysis

The baseline characteristics of patients with KTD and those without tubular dysfunction were compared by the Student's *t* test for continuous variables (e.g., kidney tubular markers), and by the χ^2 test or Fisher's exact test for categorical variables. Box plots were constructed for tubular markers of KTD and non-KTD. Diagnostic test comparison was performed using KTD as the dichotomous variable. Receiver operating characteristic (ROC) curves were constructed for individual markers, and the area under the curve (AUC) was estimated with 95 % confidence interval. The differences between the largest AUC and each of the other AUCs were tested using a nonparametric method [31], and multiple comparisons were adjusted with the Bonferroni correction. The cutoff value for each tubular marker was determined using raw data of 100 % sensitivity with maximal specificity because this point would diagnose all KTD cases with minimal false positives. For reference, two methods commonly applied for the identification of optimal cutoff points using the ROC curve were also applied: method 1 [the point on the curve closest to the point with sensitivity of one and one minus specificity of zero, calculated as the minimal value for $(1 - \text{sensitivity})^2 + (1 - \text{specificity})^2$]; and method 2 [the maximum vertical distance between the ROC curve and the diagonal line, calculated as the maximum value for (sensitivity + specificity − 1)] [32]. A *p* value <0.05 was considered statistically significant. Nonparametric methods to compare AUC of tubular makers were performed with Stata software SE ver. 12 (College Station, TX, USA). All other statistical analyses were performed with the Statistical Package for Social Sciences ver. 17.0 (SPSS, Chicago, IL, USA).

Results

A total of 190 patients were enrolled from whom blood and urine samples available for analysis (Fig. 1). Among them, 19 patients (10 %) fulfilled the criteria for KTD. The baseline characteristics and laboratory data for patients

Fig. 1 Patient enrollment. *DRV/r* ritonavir-boosted darunavir; *TDF/FTC* tenofovir/ emtricitabine; *ALT* alanine transaminase; *ULN* upper limit of normal

Japanese patients on once-daily
DRV/r plus TDF/FTC for >4 weeks
n=244

Excluded n=54
Did not consent   n=34
HIV viral load >200 copies/ml   n=6
Diabetes mellitus   n=4
ALT 2.5 times > ULN   n=1
Did not visit during study period   n=9

Enrolled in the study n=190

Patients with normal kidney tubular function   n=171
Patients with kidney tubular dysfunction   n=19

with KTD and patients without tubular dysfunction are listed in Table 1. Patients with KTD were older ($p < 0.001$), had a lower body weight ($p = 0.006$) and lower eGFR ($p = 0.003$), and were more likely to be hypertensive than patients with normal tubular function, although the difference was not significant ($p = 0.088$). The median duration of tenofovir therapy was 71.5 weeks [interquartile range (IQR), 36.8–109.2 weeks] for the entire study population and was not different between the two groups ($p = 0.888$).

Differences in tubular markers between patients with KTD and those without KTD are shown in Table 1 and box-and-whisker plots in Fig. 2. Patients with KTD had higher levels of all five tubular markers with p value <0.001 (Fig. 2). The performance of each tubular marker in differentiating patients with KTD from those with normal tubular function is illustrated by ROC curves (Fig. 3a). The AUCs and 95 % confidence intervals for the diagnosis of KTD by each tubular marker were β2M, 0.970 (0.947–0.992); α1M, 0.968 (0.944–0.992); NAG, 0.901 (0.828–0.974); FE$_{IP}$, 0.757 (0.607–0.907); and FE$_{UA}$, 0.762 (0.653–0.872). Results of comparisons of AUCs of β2M (with the largest AUC) and other markers are shown in Fig. 3b. The AUCs of β2M and α1M were not significantly different, whereas the AUCs of both FE$_{IP}$ and FE$_{UA}$ were significantly smaller than that of β2M. The AUC of NAG was marginally smaller than that of β2M with a single test, but the difference was no longer significant after adjustment of Bonferroni correction (Fig. 3b). Thus, urinary β2M and α1M had the best diagnostic performances for detecting KTD.

Identifying optimal cutoff point for tubular markers

The cutoff values for the different tubular markers with 100 % sensitivity and the maximal specificity were as follows: β2M, 1,123.2 μg/g Cr (specificity, 89 %); α1M, 15.4 mg/g Cr (specificity, 87 %); NAG, 3.58 U/g Cr (specificity, 46 %); FE$_{IP}$, 1.02 % (specificity, 0 %); and FE$_{UA}$, 3.92 % (specificity, 12 %) (Table 2). The cutoff values determined by the aforementioned two conventional methods are also listed in Table 2. The cutoff values of both β2M and α1M by method 1 yielded the high diagnostic accuracy (β2M, 1,612 μg/g Cr, sensitivity 95 %, specificity 93 %; α1M, 16.5 mg/g Cr, sensitivity 95 %, specificity 90 %), whereas the cutoff values for these two markers calculated with method 2 were the same as the aforementioned ones with 100 % sensitivity and maximal specificity. Methods 1 and 2 yielded the same cutoff value for NAG of 5.96 U/g Cr (sensitivity 90 %, specificity 86 %). For FE$_{IP}$ and FE$_{UA}$, the sensitivity was relatively low with the cutoffs gained with method 1 and method 2, suggesting that FE$_{IP}$ and FE$_{UA}$ are not useful for screening KTD (Table 2).

Table 1 Characteristics of patients with and without kidney tubular dysfunction (KTD)

	KTD (n = 19)	Non-KTD (n = 171)	p value
Kidney tubular markers			
β2M > 1,000 μg/g Cr, n (%)	19 (100)	21 (12.3)	<0.001
α1M > 16.6 mg/g Cr, n (%)	18 (94.7)	17 (9.9)	<0.001
NAG > 5.93 U/g Cr, n (%)	17 (89.5)	23 (13.5)	<0.001
Fractional excretion of phosphate >18 %, n (%)	5 (26.3)	2 (1.2)	<0.001
Fractional excretion of uric acid >15 %, n (%)	2 (10.5)	4 (2.3)	0.112
Characteristics			
Sex (male), n (%)	18 (94.7)	166 (97.1)	0.473
Age (years)[a]	60 (41–62)	38 (32–42)	<0.001
Route of transmission (homosexual contact), n (%)	16 (84.2)	153 (89.5)	0.528
Weight (kg)[a]	56 (53.5–66.5)	67.2 (58.1–75)	0.006
eGFR (ml/min/ 1.73 m²)[a]	75.5 (62.8–93.5)	87.7 (77.5–98)	0.003
Serum creatinine (mg/dl)[a]	0.85 (0.68–0.96)	0.80 (0.73–0.88)	0.168
CD4 cell count (/μl)[a]	380 (194–501)	379 (275–533)	0.261
Serum phosphate (mg/dl)[a]	3.4 (2.7–3.7)	3.2 (2.9–3.6)	0.815
Serum uric acid (mg/dl)[a]	4.7 (4.2–5.7)	5.6 (4.8–6.4)	0.080
Nephrotoxic drugs, n (%)	2 (10.5)	12 (7.0)	0.420
Hepatitis C, n (%)	0 (0)	3 (1.8)	0.728
Hepatitis B, n (%)	2 (10.5)	24 (14)	0.501
Dyslipidemia, n (%)	4 (21.1)	54 (31.6)	0.253
Hypertension, n (%)	8 (42.1)	42 (24.6)	0.088
C-reactive protein (mg/dl)[a]	0.07 (0.03–0.28)	0.07 (0.03–0.16)	0.277
TDF, weeks[a]	60.3 (17.7–115.4)	73.3 (37.7–109.1)	0.888

KTD kidney tubular dysfunction, *β2M* urinary β2-microglobulin, *α1M* urinary α1-microglobulin, *NAG* N-acetyl-β-D-glucosaminidase in urine, *FE$_{IP}$* fractional excretion of phosphate, *FE$_{UA}$* fractional excretion of uric acid, *eGFR* estimated glomerular filtration rate, *TDF* tenofovir disoproxil fumarate
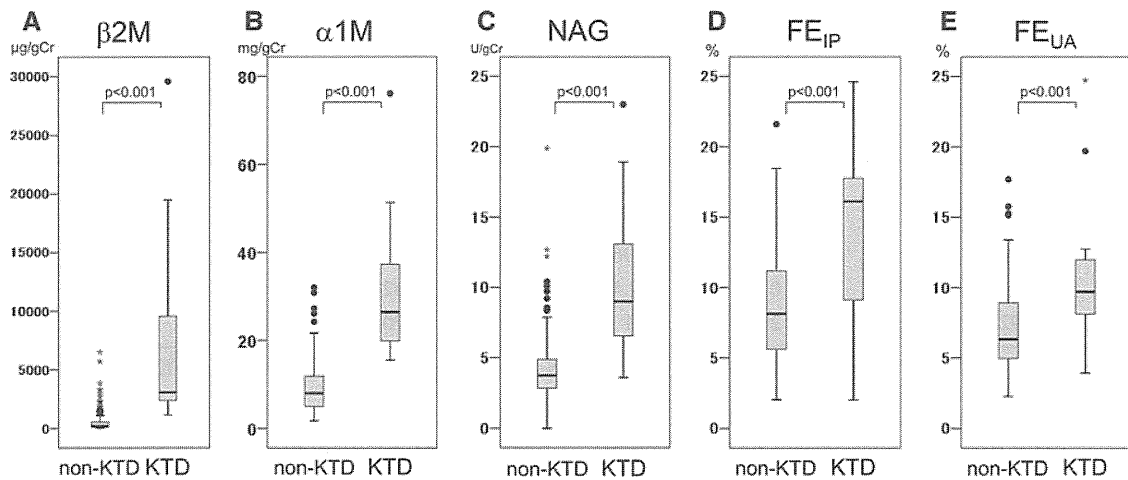
[a] Median (interquartile range)

Springer

Fig. 2 Box-and-whisker plots of five tubular markers: urinary β2-microglobulin (*β2M*) (**a**), urinary α1-microglobulin (*α1M*) (**b**), *N*-acetyl-β-D-glucosaminidase in urine (*NAG*) (**c**), fractional excretion of phosphate (*FE*$_{IP}$) (**d**), and fractional excretion of uric acid (*FE*$_{UA}$) levels in patients with kidney tubular function (*KTD*) and those with normal tubular function (*non-KTD*) (**e**). In these plots, *lines within the* *boxes* represent median values; the *upper* and *lower lines of the boxes* represent the 25th and 75th percentiles, respectively; and the *upper and lower bars outside the boxes* represent the maximum and the minimum values or to the most extreme values within 1.5 interquartile ranges of the quartiles, respectively. *Closed circles* and *asterisks* in each graph represent outliers

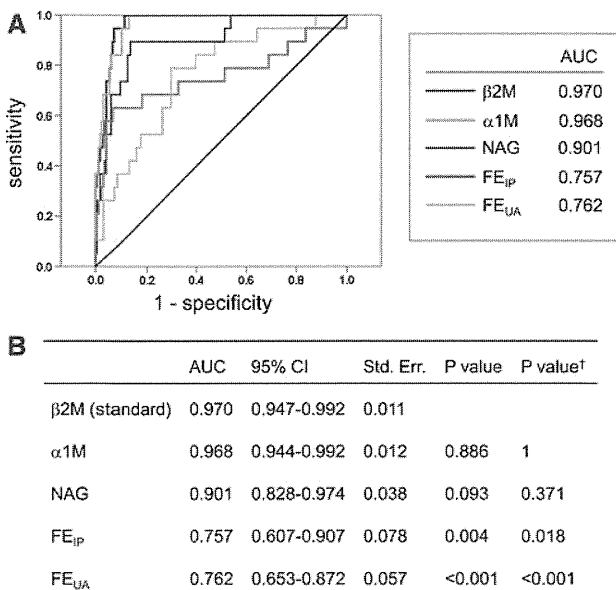|	AUC	95% CI	Std. Err.	P value	P value†
β2M (standard)	0.970	0.947-0.992	0.011		
α1M	0.968	0.944-0.992	0.012	0.886	1
NAG	0.901	0.828-0.974	0.038	0.093	0.371
FE$_{IP}$	0.757	0.607-0.907	0.078	0.004	0.018
FE$_{UA}$	0.762	0.653-0.872	0.057	<0.001	<0.001

Fig. 3 The diagnostic accuracy of five tubular markers for tenofovir-induced tubulopathy. **a** Receiver operating characteristic (ROC) curves and areas under the curve (AUC) for five tubular markers. **b** The differences between the largest AUC (β2M) and each of the other AUCs were tested using a nonparametric method. *p* value†, value adjusted with Bonferroni correction

Discussion

To our knowledge, this is the first study to compare various kidney tubular markers for screening tenofovir-induced KTD in patients with HIV-1 infection. Both urinary β2M

and α1M were identified as good screening markers with high diagnostic accuracy among the five tubular markers examined in this study. With a cutoff value of 1,123 µg/g Cr for β2M (sensitivity 100 %, specificity 89 %) and 15.4 mg/g Cr for α1M (sensitivity 100 %, specificity 87 %), these two markers are potentially suited for screening tenofovir-induced KTD. Although these low molecular weight proteins offered good screening ability, both FE$_{IP}$ and FE$_{UA}$, which are traditional tubular function markers often used for the diagnosis of Fanconi syndrome, were not useful for screening KTD. NAG, a lysosomal enzyme of proximal tubular epithelial cells, had good diagnostic accuracy with a cutoff value of 5.96 U/g Cr (sensitivity 90 %, specificity 86 %). However, with cutoff of 3.58 U/g Cr, which yields 100 % sensitivity and maximal specificity, NAG had relatively low specificity of 46 %, and thus has a high false-positive rate.

TDF is one of the most important and widely used agents in the treatment of HIV-1 infection, as well as hepatitis B infection [4]. Fixed-dose tenofovir/emtricitabine is the only preferred NRTI in the American Department of Health and Human Services (DHHS) Guidelines and the revised British HIV Association Guidelines [33, 34]. TDF is also increasingly used in resource-limited settings, following the revised 2010 WHO guidelines that recommend TDF as one of the components of first-line therapies [35]. Although tenofovir nephrotoxicity is considered to be mild and tolerable [9], its long-term consequences are unknown. Thus, it is important to have a useful screening tool for tenofovir-induced nephrotoxicity.

Table 2 Cutoff values of five kidney tubular markers (calculated with 100 % sensitivity and maximal specificity) and two conventional methods

	Cutoff with 100 % sensitivity			Method 1			Method 2		
	Cutoff	Sensitivity (%)	Specificity (%)	Cutoff	Sensitivity (%)	Specificity (%)	Cutoff	Sensitivity (%)	Specificity (%)
β2M (μg/g Cr)	1,123	100	89	1,612	95	93	1,123	100	89
α1M (mg/g Cr)	15.4	100	87	16.5	95	90	15.4	100	87
NAG (U/g Cr)	3.58	100	46	5.96	90	86	5.96	90	86
FE_{IP} (%)	1.02	100	0	12.4	68	82	14.4	63	94
FE_{UA} (%)	3.92	100	12	8.1	79	70	8.1	79	70

β2M urinary β2-microglobulin, *α1M* urinary α1-microglobulin, *NAG* N-acetyl-β-D-glucosaminidase in urine, FE_{IP} fractional excretion of phosphate, FE_{UA} fractional excretion of uric acid

Previous studies identified old age, low body weight, preexisting renal impairment, concomitant use of nephrotoxic medications, concomitant use of ritonavir-boosted protease inhibitors, advanced HIV infection (low CD4 counts, AIDS), and other comorbidities (diabetes mellitus, hypertension, hepatitis C co-infection) as risk factors for tenofovir-induced reduction in renal function [14, 27–30]. The DHHS Guidelines recommend monitoring eGFR, urinalysis, and electrolytes in patients on TDF [33]. We suggest monitoring either urinary β2M or α1M in addition to the variables recommended by the DHHS guidelines every 6 months in patients under tenofovir use, especially in those with the aforementioned risk factors in resource-rich settings.

One of the strengths of the present study is the exclusion of factors that could otherwise predispose to KTD other than tenofovir, such as active infection, diabetes mellitus, preexisting renal impairment, and HIV-1 viremia, to make prevalence of KTD lower than that in the real-world settings [20]. The cutoff values of tubular markers for screening tenofovir-induced KTD with 100 % sensitivity were calculated in this setting. Thus, in applying these cutoff values in clinical practice with high prevalence rates of KTD, the false-positive rate will be lower than the one reported in the present study, making these cutoff values even more useful.

Another strength of the study is that the enrolled patients were on the same antiretroviral regimen (once-daily ritonavir-boosted darunavir plus fixed-dose tenofovir/emtricitabine). This practice helped proper evaluation of the diagnostic accuracy of the five tubular markers, because plasma concentrations of tenofovir and severity of tenofovir-induced KTD are influenced by concomitant use of antiretrovirals, and the delta change in plasma tenofovir concentration likely differs in the presence of each concomitant drug [36]. Thus, by enrolling patients on the same antiretroviral combination, this study excluded an important confounding factor for tenofovir-induced KTD.

Both β2M and α1M are low molecular weight proteins (<40 kDa) used as markers of kidney tubular function.

β2M and the free unbound form of α1M are freely filtered by the glomerulus and reabsorbed almost completely in proximal tubular cells [37]. Serum β2M has been used as a surrogate marker of inflammation, because it is expressed on the surface of most nucleated cells, as part of class I major histocompatibility complex. On the other hand, α1M is mainly produced in the liver, and although its function is not fully understood, it has antioxidant properties and acts as a radical scavenger [38]. Of note, technical difficulty has been reported in the measurement of both markers; for β2M, acidic urine with pH <6.0 causes time- and temperature-dependent degradation of β2M [39]. Urinary α1M is more stable than β2M when stored in acidic urine; however, diurnal variation and gender differences have been reported [40–42].

There are several limitations in this study. First, there is no gold standard definition for KTD. The collection of abnormal tubular markers was used as a reference standard in this study, following their use in previous studies for the diagnosis of KTD [17, 43]. However, the criteria used for the diagnosis of KTD in each previous study included haphazard combination of tubular markers [16, 44]. Accordingly, this study selected five markers (β2M, α1M, NAG, FE_{IP}, and FE_{UA}) after taking into consideration their availability and cost. Thus, our study did not investigate other tubular markers, such as γ-glutamyl transpeptidase, retinol binding protein, and neutrophil gelatinase-associated lipocalin. Second, although this study evaluated the diagnostic values for five variables (β2M, α1M, NAG, FE_{IP}, and FE_{UA}), these variables were not fully independent from KTD, the reference standard, because KTD was defined as the collection of abnormal tubular markers [17, 43]. Third, the study subjects were mostly men, and thus the results of this study are not necessarily applicable to women, especially considering that gender variation should be taken into account in evaluation of α1M [40].

In conclusion, the present study identified urinary β2M and α1M as highly useful screening markers for tenofovir-induced KTD, in a setting designed to exclusively evaluate tenofovir-induced KTD. In the assessment of renal function

in patients under tenofovir therapy, regular monitoring of either urinary β2M or α1M, in addition to urinalysis, serum creatinine, and electrolytes, should be helpful in the diagnosis of early-stage tenofovir-induced KTD. Screening for tenofovir-induced KTD is especially important in patients with several risk factors for KTD, because undetected long-term tubular dysfunction might lead to premature osteopenia caused by phosphate wasting, and accelerated progression of renal dysfunction, both of which could result in a serious outcome.

References

1. Sax PE, Tierney C, Collier AC, Daar ES, Mollan K, Budhathoki C, et al. Abacavir/lamivudine versus tenofovir DF/emtricitabine as part of combination regimens for initial treatment of HIV: final results. J Infect Dis. 2011;204:1191–201.
2. Post FA, Moyle GJ, Stellbrink HJ, Domingo P, Podzamczer D, Fisher M, et al. Randomized comparison of renal effects, efficacy, and safety with once-daily abacavir/lamivudine versus tenofovir/emtricitabine, administered with efavirenz, in antiretroviral-naive, HIV-1-infected adults: 48-week results from the ASSERT study. J Acquir Immune Defic Syndr. 2010;55:49–57.
3. Arribas JR, Pozniak AL, Gallant JE, Dejesus E, Gazzard B, Campo RE, et al. Tenofovir disoproxil fumarate, emtricitabine, and efavirenz compared with zidovudine/lamivudine and efavirenz in treatment-naive patients: 144-week analysis. J Acquir Immune Defic Syndr. 2008;47:74–8.
4. Woo G, Tomlinson G, Nishikawa Y, Kowgier M, Sherman M, Wong DK, et al. Tenofovir and entecavir are the most effective antiviral agents for chronic hepatitis B: a systematic review and Bayesian meta-analyses. Gastroenterology. 2010;139:1218–29.
5. Verhelst D, Monge M, Meynard JL, Fouqueray B, Mougenot B, Girard PM, et al. Fanconi syndrome and renal failure induced by tenofovir: a first case report. Am J Kidney Dis. 2002;40:1331–3.
6. Schaaf B, Aries SP, Kramme E, Steinhoff J, Dalhoff K. Acute renal failure associated with tenofovir treatment in a patient with acquired immunodeficiency syndrome. Clin Infect Dis. 2003;37:e41–3.
7. Peyriere H, Reynes J, Rouanet I, Daniel N, de Boever CM, Mauboussin JM, et al. Renal tubular dysfunction associated with tenofovir therapy: report of 7 cases. J Acquir Immune Defic Syndr. 2004;35:269–73.

8. Nishijima T, Gatanaga H, Komatsu H, Tsukada K, Shimbo T, Aoki T, et al. Renal function declines more in tenofovir- than abacavir-based antiretroviral therapy in low-body weight treatment-naive patients with HIV infection. PLoS ONE. 2012;7:e29977.
9. Cooper RD, Wiebe N, Smith N, Keiser P, Naicker S, Tonelli M. Systematic review and meta-analysis: renal safety of tenofovir disoproxil fumarate in HIV-infected patients. Clin Infect Dis. 2010;51:496–505.
10. Fux CA, Rauch A, Simcock M, Bucher HC, Hirschel B, Opravil M, et al. Tenofovir use is associated with an increase in serum alkaline phosphatase in the Swiss HIV cohort study. Antivir Ther. 2008;13:1077–82.
11. McComsey GA, Kitch D, Daar ES, Tierney C, Jahed NC, Tebas P, et al. Bone mineral density and fractures in antiretroviral-naive persons randomized to receive abacavir-lamivudine or tenofovir disoproxil fumarate-emtricitabine along with efavirenz or atazanavir-ritonavir: AIDS Clinical Trials Group A5224s, a substudy of ACTG A5202. J Infect Dis. 2011;203:1791–801.
12. Gallant JE, Winston JA, DeJesus E, Pozniak AL, Chen SS, Cheng AK, et al. The 3-year renal safety of a tenofovir disoproxil fumarate vs. a thymidine analogue-containing regimen in antiretroviral-naive patients. AIDS. 2008;22:2155–63.
13. Izzedine H, Hulot JS, Vittecoq D, Gallant JE, Staszewski S, Launay-Vacher V, et al. Long-term renal safety of tenofovir disoproxil fumarate in antiretroviral-naive HIV-1-infected patients. Data from a double-blind randomized active-controlled multicentre study. Nephrol Dial Transplant. 2005;20:743–6.
14. Gatanaga H, Tachikawa N, Kikuchi Y, Teruya K, Genka I, Honda M, et al. Urinary beta2-microglobulin as a possible sensitive marker for renal injury caused by tenofovir disoproxil fumarate. AIDS Res Hum Retroviruses. 2006;22:744–8.
15. Papaleo A, Warszawski J, Salomon R, Jullien V, Veber F, Dechaux M, et al. Increased beta-2 microglobulinuria in human immunodeficiency virus-1-infected children and adolescents treated with tenofovir. Pediatr Infect Dis J. 2007;26:949–51.
16. Han WK, Wagener G, Zhu Y, Wang S, Lee HT. Urinary biomarkers in the early detection of acute kidney injury after cardiac surgery. Clin J Am Soc Nephrol. 2009;4:873–82.
17. Izzedine H, Hulot JS, Villard E, Goyenvalle C, Dominguez S, Ghosn J, et al. Association between ABCC2 gene haplotypes and tenofovir-induced proximal tubulopathy. J Infect Dis. 2006;194:1481–91.
18. Rodriguez-Novoa S, Labarga P, Soriano V, Egan D, Albalater M, Morello J, et al. Predictors of kidney tubular dysfunction in HIV-infected patients treated with tenofovir: a pharmacogenetic study. Clin Infect Dis. 2009;48:e108–16.
19. Han WK, Waikar SS, Johnson A, Betensky RA, Dent CL, Devarajan P, et al. Urinary biomarkers in the early diagnosis of acute kidney injury. Kidney Int. 2008;73:863–9.
20. Ando M, Yanagisawa N, Ajisawa A, Tsuchiya K, Nitta K. Kidney tubular damage in the absence of glomerular defects in HIV-infected patients on highly active antiretroviral therapy. Nephrol Dial Transplant. 2011;26:3224–9.
21. Bossuyt PM, Reitsma JB, Bruns DE, Gatsonis CA, Glasziou PP, Irwig LM, et al. Towards complete and accurate reporting of studies of diagnostic accuracy: the STARD Initiative. Ann Intern Med. 2003;138:40–4.
22. Nishijima T, Komatsu H, Higasa K, Takano M, Tsuchiya K, Hayashida T, et al. Single nucleotide polymorphisms in ABCC2 associate with tenofovir-induced kidney tubular dysfunction in Japanese patients with HIV-1 infection: a pharmacogenetic study. Clin Infect Dis. 2012;55(11):1558–67.
23. Cockcroft DW, Gault MH. Prediction of creatinine clearance from serum creatinine. Nephron. 1976;16:31–41.
24. Carrieri M, Trevisan A, Bartolucci GB. Adjustment to concentration-dilution of spot urine samples: correlation between

specific gravity and creatinine. Int Arch Occup Environ Health. 2001;74:63–7.

25. Salem MA, el-Habashy SA, Saeid OM, el-Tawil MM, Tawfik PH. Urinary excretion of *N*-acetyl-beta-D-glucosaminidase and retinol binding protein as alternative indicators of nephropathy in patients with type 1 diabetes mellitus. Pediatr Diabetes. 2002;3: 37–41.

26. Ezinga M, Wetzels J, van der Ven A, Burger D. Kidney tubular dysfunction is related to tenofovir plasma concentration (abstract 603). In: Program and abstracts of the 19th Conference on Retroviruses and Opportunistic Infections, 5–8 March, 2012, Seattle, WA

27. Gupta SK, Eustace JA, Winston JA, Boydstun II, Ahuja TS, Rodriguez RA, et al. Guidelines for the management of chronic kidney disease in HIV-infected patients: recommendations of the HIV Medicine Association of the Infectious Diseases Society of America. Clin Infect Dis. 2005;40:1559–85.

28. Goicoechea M, Liu S, Best B, Sun S, Jain S, Kemper C, et al. Greater tenofovir-associated renal function decline with protease inhibitor-based versus nonnucleoside reverse-transcriptase inhibitor-based therapy. J Infect Dis. 2008;197:102–8.

29. Nelson MR, Katlama C, Montaner JS, Cooper DA, Gazzard B, Clotet B, et al. The safety of tenofovir disoproxil fumarate for the treatment of HIV infection in adults: the first 4 years. AIDS. 2007;21:1273–81.

30. Fernandez-Fernandez B, Montoya-Ferrer A, Sanz AB, Sanchez-Nino MD, Izquierdo MC, Poveda J, et al. Tenofovir nephrotoxicity: 2011 update. AIDS Res Treat. 2011;2011:354908.

31. DeLong ER, DeLong DM, Clarke-Pearson DL. Comparing the areas under two or more correlated receiver operating characteristic curves: a nonparametric approach. Biometrics. 1988;44: 837–45.

32. Perkins NJ, Schisterman EF. The inconsistency of "optimal" cutpoints obtained using two criteria based on the receiver operating characteristic curve. Am J Epidemiol. 2006;163:670–5.

33. Panel on Antiretroviral Guidelines for Adults and Adolescents. Guidelines for the use of antiretroviral agents in HIV-1-infected adults and adolescents. Department of Health and Human Services. 1–239. Available at http://www.aidsinfo.nih.gov/Content Files/AdultandAdolescentGL.pdf. Accessed 7 June 2012.

34. The BHIVA Treatment Guidelines Writing Group. BHIVA guidelines for the treatment of HIV-1 positive adults with antiretroviral therapy 2012. British HIV Association. 1–139. Available at http://www.bhiva.org/documents/Guidelines/Treatment/2012/120430TreatmentGuidelines.pdf. Accessed 15 June 2012.

35. Antiretroviral therapy for HIV infection in adults and adolescents Recommendations for a public health approach 2010 revision. World Health Organization. 1–156. Available at http://whqlibdoc.who.int/publications/2010/9789241599764_eng.pdf. Accessed 7 June 2012.

36. Kiser JJ, Carten ML, Aquilante CL, Anderson PL, Wolfe P, King TM, et al. The effect of lopinavir/ritonavir on the renal clearance of tenofovir in HIV-infected patients. Clin Pharmacol Ther. 2008;83:265–72.

37. Lisowska-Myjak B. Serum and urinary biomarkers of acute kidney injury. Blood Purif. 2010;29:357–65.

38. Olsson MG, Centlow M, Rutardottir S, Stenfors I, Larsson J, Hosseini-Maaf B, et al. Increased levels of cell-free hemoglobin, oxidation markers, and the antioxidative heme scavenger alpha(1)-microglobulin in preeclampsia. Free Radic Biol Med. 2010;48:284–91.

39. Hong CY, Chia KS. Markers of diabetic nephropathy. J Diabetes Complications. 1998;12:43–60.

40. Andersson L, Haraldsson B, Johansson C, Barregard L. Methodological issues on the use of urinary alpha-1-microglobuline in epidemiological studies. Nephrol Dial Transplant. 2008;23: 1252–6.

41. Tencer J, Thysell H, Andersson K, Grubb A. Long-term stability of albumin, protein HC, immunoglobulin G, kappa- and lambda-chain-immunoreactivity, orosomucoid and alpha 1-antitrypsin in urine stored at −20 degrees C. Scand J Urol Nephrol. 1997;31: 67–71.

42. Itoh Y, Kawai T. Human alpha 1-microglobulin: its measurement and clinical significance. J Clin Lab Anal. 1990;4:376–84.

43. Rodriguez-Novoa S, Labarga P, Soriano V. Pharmacogenetics of tenofovir treatment. Pharmacogenomics. 2009;10:1675–85.

44. Rodriguez-Novoa S, Alvarez E, Labarga P, Soriano V. Renal toxicity associated with tenofovir use. Expert Opin Drug Saf. 2010;9:545–59.

INTERNAL MEDICINE

Idiopathic Oropharyngeal and Esophageal Ulcers Related to HIV Infection Successfully Treated with Antiretroviral Therapy Alone

Yohei Hamada[1], Naoyoshi Nagata[2], Haruhito Honda[1], Katsuji Teruya[1],
Hiroyuki Gatanaga[1], Yoshimi Kikuchi[1] and Shinichi Oka[1]

Abstract

We herein report the case of an HIV-positive man who was diagnosed with idiopathic esophageal and oropharyngeal ulceration. The esophageal and oropharyngeal ulcers were considered to be idiopathic and related to HIV infection after excluding the possibility of infection with known pathogens. Both the esophageal and oropharyngeal ulcers showed significant improvements following antiretroviral therapy alone. Idiopathic esophageal ulcers are a well-known complication of late-stage HIV infection. However, involvement of both the esophagus and pharynx is rare. Furthermore, antiretroviral therapy without concomitant steroids is effective against idiopathic esophageal and oropharyngeal ulcers related to HIV infection.

Key words: HIV infection, idiopathic esophageal ulcer, pharyngeal ulcer, antiretroviral therapy, gastrointestinal diseases

Introduction

Esophageal ulceration is a common complication in patients with human immunodeficiency virus-1 (HIV) infection, especially in the late stage. Although esophageal ulcerations can be caused by various infectious agents, such as *Candida* species, cytomegalovirus (CMV) and herpes simplex virus (HSV), a large proportion of patients are diagnosed with idiopathic esophageal ulcerations (1, 2) with no detectable etiology. Oropharyngeal ulcers are also an important comorbidity that can become progressive in HIV-infected patients (3, 4). The common infectious agents of esophageal ulcerations are known to also cause oropharyngeal ulcerations, although some cases are considered idiopathic with no identifiable etiology (5, 6). However, simultaneous involvement of the esophagus and oropharynx is uncommon outside of HSV esophagitis (5). We herein report a case of unusual discrete ulcers of the oropharynx and esophagus in a patient with HIV infection that showed a rapid improvement following treatment with antiretroviral therapy alone.

Case Report

A previously healthy 60-year-old Japanese homosexual man presented with severe odynophagia. He was diagnosed with oral candidiasis and HIV infection and therefore had been referred to our hospital (day-1). Laboratory tests showed a low CD4+ cell count (49/μL), a high HIV-RNA titer (1.0×10^6 copies/mL) and a low serum albumin level (Alb 2.9 g/dL). Whole-blood polymerase chain reaction (PCR) was negative for both CMV and HSV. The patient was treated with fluconazole for seven days for suspected esophageal candidiasis. Despite this treatment, the odynophagia did not improve. Since oral ulcers were noticed, treatment with oral valaciclovir at a dose of 1,000 mg/ day was initiated based on a presumptive diagnosis of HSV infection. However, the odynophagia persisted, and the oral ulcers did not show any improvement despite a 3-week
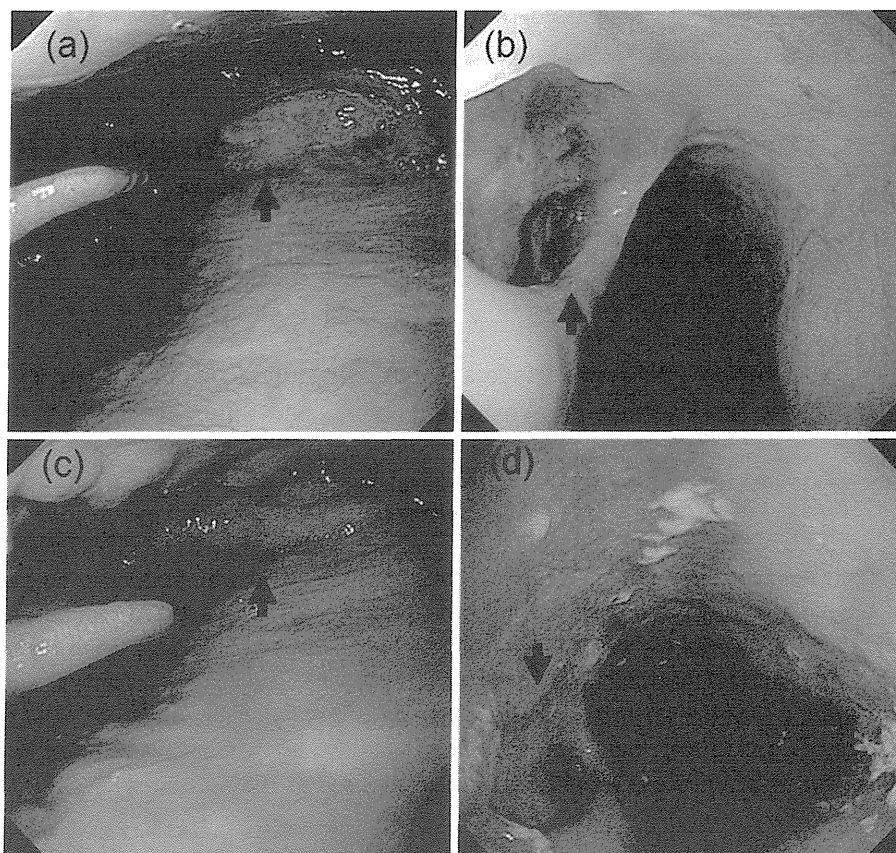
Figure.   Endoscopic findings of the pharynx and esophagus. The pharyngeal (a) and esophageal (b) ulcers before the administration of antiretroviral therapy. The endoscopic appearance of the pharynx (c) and esophagus (d) on day 22 of antiretroviral therapy. Black arrows: ulcers.

course of anti-HSV therapy; thus, upper gastrointestinal endoscopy was performed. Endoscopy showed large, discrete and well-circumscribed esophageal and pharyngeal ulcers (Figure a, b). Because a diagnosis of CMV esophagitis was suspected based on the endoscopic appearance of the ulcers, treatment with intravenous gancicrovir at a dose of 5 mg/kg every 12 hours was initiated and the valaciclovir was discontinued. However, a histopathological examination of the biopsy specimen obtained from the base and edge of an ulcer before the initiation of gancicrovir therapy revealed lymphocytic infiltration without intranuclear or intracytoplasmic inclusion bodies. Immunohistochemical staining for CMV and HSV was negative. PCR assays of both pharyngeal and esophageal biopsies were negative for CMV-DNA and HSV-DNA ($\leq$40 copies/μg DNA). Furthermore, repeat endoscopy performed after two weeks of gancicrovir therapy showed exacerbation of the ulcers. Based on these findings, we administered antiretroviral therapy consisting of ritonavir-boosted darunavir with abacavir/lamivudine. The gancicrovir therapy was discontinued after the completion of a 3-week course of treatment. The odynophagia gradually improved and ultimately disappeared two weeks later, while the CD4 count increased to 91/μL and the HIV-RNA titer decreased to 4×10^4 copies/mL. Endoscopy performed on day 22 of antiretroviral therapy demonstrated significant reductions in the size and depth of the pharyngeal and esophageal ulcers (Fig-

ure c, d). Additionally, resolution of the oral ulcers was noticed.

Discussion

To our knowledge, this is the first report of idiopathic esophageal and oropharyngeal ulcers successfully treated with antiretroviral therapy alone in a patient with late-stage HIV infection. Steroids are commonly used as the standard treatment for idiopathic esophageal ulcers (2, 7). However, steroids can lead to serious opportunistic infections due to their immunosuppressive effects. The efficacy of steroids is mostly based on reports from the pre-highly active antiretroviral therapy era, and the efficacy of antiretroviral therapy has not been examined. As described above, steroid therapy may not be necessary when a potent combination of antiretroviral therapy is administered. The etiology of idiopathic esophageal ulcers is still not fully understood. Although such ulcers are considered to be associated with HIV infection, they have been referred to as idiopathic when no identifiable etiologic agent other than HIV infection is present (8, 9). The potential pathogenesis of these ulcers includes apoptosis of the esophageal mucosa induced by HIV infection (10). Based on this probable pathogenesis, it is therefore considered to be rational to administer antiretroviral therapy to treat idiopathic esophageal ulcers.

The diagnosis of idiopathic oropharyngeal and esophageal ulcers is established by excluding other infectious agents known to cause esophageal ulceration, including CMV, HSV and *Candida* sp, by performing histopathological and immunological examinations of biopsy specimens (1, 2, 5, 6). In our case, the histopathological findings showed no evidence of any infectious pathogens, and CMV and HSV infection were also excluded by PCR assays, which have a high sensitivity (11, 12). Furthermore, the oropharyngeal and esophageal ulcers were refractory to anti-CMV and anti-HSV therapy. In addition, the ulcers showed significant improvement following the administration of antiretroviral therapy alone. Therefore, the final diagnosis was idiopathic oropharyngeal and esophageal ulcers related to HIV infection.

Involvement of both the oropharynx and esophagus in HSV-related ulcers is not uncommon (5). However, in our patient, the esophageal and oropharyngeal ulcers were considered idiopathic, which is extremely rare. In this case, the ulcers in both regions were examined endoscopically. Therefore, performing careful endoscopic examinations of not only the esophagus, but also the pharynx, is considered to be important for establishing the cause of odynophagia in HIV-infected patients.

In conclusion, a pharyngeal and esophageal biopsy obtained using upper gastrointestinal endoscopy was useful for establishing the diagnosis in this case. Furthermore, antiretroviral therapy alone resulted in a significant improvement of the idiopathic ulcers in our HIV-infected patient. The initiation of antiretroviral therapy without steroids is therefore a reasonable option for treating idiopathic oropharyngeal and esophageal ulcers in HIV-infected patients.

The authors state that they have no Conflict of Interest (COI).

References

1. Bonacini M, Young T, Laine L. The causes of esophageal symptoms in human immunodeficiency virus infection. A prospective study of 110 patients. Arch Intern Med **151**: 1567-1572, 1991.
2. Wilcox CM, Schwartz DA, Clark WS. Esophageal ulceration in human immunodeficiency virus infection. Causes, response to therapy, and long-term outcome. Ann Intern Med **123**: 143-149, 1995.
3. Gorin I, Vilette B, Gehanno P, Escande JP. Thalidomide in hyperalgic pharyngeal ulceration of AIDS. Lancet **335**: 1343, 1990.
4. MacPhail LA, Greenspan D, Feigal DW, Lennette ET, Greenspan JS. Recurrent aphthous ulcers in association with HIV infection. Description of ulcer types and analysis of T-lymphocyte subsets. Oral Surg Oral Med Oral Pathol **71**: 678-683, 1991.
5. Wilcox CM, Straub RF, Clark WS. Prospective evaluation of oropharyngeal findings in human immunodeficiency virus-infected patients with esophageal ulceration. Am J Gastroenterol **90**: 1938-1941, 1995.
6. Liang GS, Daikos GL, Serfling U, et al. An evaluation of oral ulcers in patients with AIDS and AIDS-related complex. J Am Acad Dermatol **29**: 563-568, 1993.
7. Wilcox CM, Schwartz DA. Comparison of two corticosteroid regimens for the treatment of HIV-associated idiopathic esophageal ulcer. Am J Gastroenterol **89**: 2163-2167, 1994.
8. Bhaijee F, Subramony C, Tang SJ, Pepper DJ. Human immunodeficiency virus-associated gastrointestinal disease: common endoscopic biopsy diagnoses. Patholog Res Int **2011**: 247923, 2011.
9. Nishijima T, Tsukada K, Nagata N, et al. Antiretroviral therapy alone resulted in successful resolution of large idiopathic esophageal ulcers in a patient with acute retroviral syndrome. AIDS **25**: 1677-1679, 2011.
10. Houghton JM, Korah RM, Kim KH, Small MB. A role for apoptosis in the pathogenesis of AIDS-related idiopathic esophageal ulcers. J Infect Dis **175**: 1216-1219, 1997.
11. Jazeron JF, Barbe C, Frobert E, et al. Virological diagnosis of herpes simplex virus 1 esophagitis by quantitative real-time PCR assay. J Clin Microbiol **50**: 948-952, 2012.
12. Reddy N, Wilcox CM. Diagnosis & management of cytomegalovirus infections in the GI tract. Expert Rev Gastroenterol Hepatol **1**: 287-294, 2007.

Yuichi Yagita, Nozomi Kuse, Kimiko Kuroki, Hiroyuki Gatanaga, Jonathan M. Carlson, Takayuki Chikata, Zabrina L. Brumme, Hayato Murakoshi, Tomohiro Akahoshi, Nico Pfeifer, Simon Mallal, Mina John, Toyoyuki Ose, Haruki Matsubara, Ryo Kanda, Yuko Fukunaga, Kazutaka Honda, Yuka Kawashima, Yasuo Ariumi, Shinichi Oka, Katsumi Maenaka and Masafumi Takiguchi

Distinct HIV-1 Escape Patterns Selected by Cytotoxic T Cells with Identical Epitope Specificity

Yuichi Yagita,[a] Nozomi Kuse,[a] Kimiko Kuroki,[b] Hiroyuki Gatanaga,[a,c] Jonathan M. Carlson,[d] Takayuki Chikata,[a] Zabrina L. Brumme,[e,f] Hayato Murakoshi,[a] Tomohiro Akahoshi,[a] Nico Pfeifer,[d] Simon Mallal,[g] Mina John,[g] Toyoyuki Ose,[b] Haruki Matsubara,[b] Ryo Kanda,[b] Yuko Fukunaga,[b] Kazutaka Honda,[a] Yuka Kawashima,[a] Yasuo Ariumi,[a] Shinichi Oka,[a,c] Katsumi Maenaka,[b] Masafumi Takiguchi[a]

Center for AIDS Research, Kumamoto University, Chuo-ku, Kumamoto, Japan[a]; Laboratory of Biomolecular Science, Faculty of Pharmaceutical Sciences, Hokkaido University, Kita-ku, Sapporo, Japan[b]; AIDS Clinical Center, National Center for Global Health and Medicine, Shinjuku-ku, Tokyo, Japan[c]; eScience Group, Microsoft Research, Los Angeles, California[d]; Faculty of Health Sciences, Simon Fraser University, Burnaby BC, Canada[e]; British Columbia Centre for Excellence in HIV/AIDS, Vancouver, BC, Canada[f]; Institute for Immunology & Infectious Diseases, Murdoch University, Murdoch, Western Australia, Australia[g]

Pol283-8-specific, HLA-B*51:01-restricted, cytotoxic T cells (CTLs) play a critical role in the long-term control of HIV-1 infection. However, these CTLs select for the reverse transcriptase (RT) I135X escape mutation, which may be accumulating in circulating HIV-1 sequences. We investigated the selection of the I135X mutation by CTLs specific for the same epitope but restricted by HLA-B*52:01. We found that Pol283-8-specific, HLA-B*52:01-restricted CTLs were elicited predominantly in chronically HIV-1-infected individuals. These CTLs had a strong ability to suppress the replication of wild-type HIV-1, though this ability was weaker than that of HLA-B*51:01-restricted CTLs. The crystal structure of the HLA-B*52:01-Pol283-8 peptide complex provided clear evidence that HLA-B*52:01 presents the peptide similarly to HLA-B*51:01, ensuring the cross-presentation of this epitope by both alleles. Population level analyses revealed a strong association of HLA-B*51:01 with the I135T mutant and a relatively weaker association of HLA-B*52:01 with several I135X mutants in both Japanese and predominantly Caucasian cohorts. An in vitro viral suppression assay revealed that the HLA-B*52:01-restricted CTLs failed to suppress the replication of the I135X mutant viruses, indicating the selection of these mutants by the CTLs. These results suggest that the different pattern of I135X mutant selection may have resulted from the difference between these two CTLs in the ability to suppress HIV-1 replication.

HIV-1-specific cytotoxic T cells (CTLs) play an important role in the control of HIV-1 replication (1–8); however, they also select immune escape mutations (9, 10). Population level adaptation of HIV to human leukocyte antigen (HLA) has been demonstrated (11–15), suggesting that HIV-1 can successfully adapt to immune responses previously effective against it.

It is well known that particular mutations can be selected by CTLs specific for a single HIV-1 epitope. On the other hand, studies on HLA-associated HIV-1 polymorphisms have revealed examples of particular mutations associated with multiple HLA class I alleles (16–21), suggesting that the same mutation can be selected by CTLs carrying different specificities in some cases. However, the selection of the same mutation by CTLs specific for different HIV-1 epitopes has rarely been reported. The change from Ala to Pro at residue 146 of Gag (A146P) is a well-analyzed case. A146P is an escape selected by not only HLA-B*57-restricted, ISW9-specific CTLs (22) but also by HLA-B*15:10-restricted and HLA-B*48:01-restricted CTLs (15, 23, 24), although the latter CTLs selected it by different mechanisms. The replacement of Thr with Asn at residue 242 (T242N) of Gag is another case. This mutant is selected by HLA-B*58:01-restricted and HLA-B*57-restricted CTLs specific for the TW10 epitope in HIV-1 clade B- and C-infected individuals (25–27).

The presence of Pol283-8(TAFTIPSI: TI8)-specific, HLA-B*51:01-restricted CTLs is associated with low viral loads in HIV-1-infected Japanese hemophiliacs, supporting an important role in the long-term control of HIV-1 infection (28). We previously showed that the frequency of a mutation at position 135 (I135X) of reverse transcriptase (RT) is strongly correlated with the prevalence of HLA-B*51 among nine cohorts worldwide and that this mutation is selected by Pol283-8(TAFTIPSI: TI8)-specific, HLA-

B*51:01-restricted CTLs (15). Of these cohorts, a Japanese one showed the highest frequency of the I135X mutation in HLA-B*51:01 negatives (66% in a Japanese cohort and 11 to 29% in other cohorts). This finding may be explained by the fact that the Japanese cohort has the highest prevalence of HLA-B*51:01 among these cohorts. Another possibility is that this mutation is selected by HIV-1-specific CTLs restricted by other HLA alleles, which are highly frequent among Japanese individuals but infrequent in or absent from other populations. To clarify the latter possibility, we first analyzed the association of the I135X mutation with other HLA class I alleles in a Japanese cohort and found this mutation also to be associated with HLA-B*52:01. We next sought to identify an HLA-B*52:01-restricted CTL epitope including RT135 and found that both HLA-B*51:01 and -B*52:01 can present the same epitope, Pol283-8. Using population level analyses of Japanese and Caucasian cohorts, we identified HLA-B*51:01- and HLA-B*52:01-specific polymorphisms at RT codon 135 (position 8 of this epitope) and characterized differential pathways of escape between these two alleles. In addition, we assessed the in vitro ability of HLA-B*52:01- and HLA-B*51:01-restricted CTLs to se-

lect I135X mutants and elucidated the crystal structure of the HLA-B*52:01-Pol283-8 peptide complex.

MATERIALS AND METHODS

Patients. Two hundred fifty-seven chronically HIV-1-infected, antiretroviral-naïve Japanese individuals were recruited for the present study, which was approved by the ethics committees of Kumamoto University and the National Center for Global Health and Medicine, Japan. Written informed consent was obtained from all subjects according to the Declaration of Helsinki.

In addition, HLA-associated immune selection pressure at RT codon 135 was investigated in the International HIV Adaptation Collaborative (IHAC) cohort, comprising >1,200 chronically HIV-infected, antiretroviral-naïve individuals from Canada, the United States, and Western Australia (19). The majority of the IHAC participants were Caucasian, and the HIV subtype distribution was >95% subtype B.

HIV-1 clones. An infectious proviral clone of HIV-1, pNL-432, and its mutant form pNL-M20A (containing a substitution of Ala for Met at residue 20 of Nef) were previously reported (29). Pol283-8 mutant viruses (Pol283-8L, -8T, -8V, and 8R) were previously generated on the basis of pNL-432 (15, 28).

Generation of CTL clones. Pol283-8-specific, HLA-B*52:01-restricted CTL clones were generated from HIV-1-specific, bulk-cultured T cells by limiting dilution in U-bottom 96-well microtiter plates (Nunc, Roskilde, Denmark). Each well contained 200 μl of the cloning mixture (about 1×10^6 irradiated allogeneic peripheral blood mononuclear cells (PBMCs) from healthy donors and 1×10^5 irradiated C1R-B*52:01 cells prepulsed with the corresponding peptide at 1 μM in RPMI 1640 supplemented with 10% human plasma and 200 U/ml human recombinant interleukin-2).

Intracellular cytokine staining (ICS) assay. PBMCs from HIV-1-seropositive HLA-B*52:01+ HLA-B*51:01− individuals were cultured with each peptide (1 μM). Two weeks later, the cultured cells were stimulated with C1R-B*52:01 cells or those prepulsed with Pol283-8 peptide (1 μM) for 60 min, and then they were washed twice with RPMI 1640 containing 10% fetal calf serum (RPMI 1640-10% FCS). Subsequently, brefeldin A (10 μg/ml) was added. After these cells had been incubated for 6 h, they were stained with an anti-CD8 monoclonal antibody (MAb; Dako Corporation, Flostrup, Denmark), fixed with 4% paraformaldehyde, and then permeabilized with permeabilization buffer. Thereafter, the cells were stained with an anti-gamma interferon (IFN-γ) MAb (BD Bioscience). The percentage of CD8+ cells positive for intracellular IFN-γ was analyzed by using a FACS-Cant II (BD Biosciences, San Jose, CA). All flow cytometric data were analyzed with FlowJo software (Tree Star, Inc., Ashland, OR).

Identification of 11-mer peptide recognized by HLA-B*52:01-restricted CD8+ T cells. We identified an 11-mer peptide recognized by HLA-B*52:01-restricted CD8+ T cells as follows. We stimulated PBMCs from a chronically HIV-1-infected HLA-B*52:01+ donor (KI-069) with a peptide cocktail including overlapping 17-mer peptides covering RT135 and cultured the cells for 14 days. The cells in bulk culture were assessed by performing an ICS assay for C1R-HLA-B*52:01 cells prepulsed with each of these 17-mer peptides. The bulk-cultured cells recognized the target cells prepulsed with two of the 17-mer peptides assessed, Pol17-47 (KDFRKYTAFTIPSINNE) and Pol17-48 (TAFTIPSINNETPGIRT). Further analysis with 11-mer overlapping peptides covering the Pol17-48 sequence showed that these bulk-cultured cells recognized the target cells prepulsed with Pol11-142 (TAFTIPSINNE) but not those prepulsed with Pol11-143 (FTIPSINNETP).

Assay of cytotoxicity of CTL clones to target cells prepulsed with the epitope peptide or infected with a vaccinia virus–HIV-1 recombinant. The cytotoxicity of Pol283-8-specific, HLA-B*52:01-restricted CTL clones to C1R cells expressing HLA-B*52:01 (C1R-B*52:01), which were previously generated (30), and prepulsed with peptide or infected with a vaccinia virus-HIV-1Gag/Pol recombinant was determined by the stan-

dard ^{51}Cr release assay described previously (31). In brief, the infected cells were incubated with 150 μCi Na$_2$^{51}CrO$_4$ in saline for 60 min and then washed three times with RPMI 1640 medium containing 10% newborn calf serum. Labeled target cells (2×10^3/well) were added to each well of a U-bottom 96-well microtiter plate (Nunc, Roskilde, Denmark) with the effector cells at an effector-to-target (E/T) cell ratio of 2:1. The cells were then incubated for 6 h at 37°C. The supernatants were collected and analyzed with a gamma counter. Spontaneous ^{51}Cr release was determined by measuring the number of counts per minute (cpm) in supernatants from wells containing only target cells (cpm spn). Maximum ^{51}Cr release was determined by measuring the cpm in supernatants from wells containing target cells in the presence of 2.5% Triton X-100 (cpm max). Specific lysis was defined as (cpm exp − cpm spn)/(cpm max − cpm spn) × 100, where cpm exp is the number of cpm in the supernatant in the wells containing both target and effector cells.

Enzyme-linked immunospot (ELISPOT) assay. Cryopreserved PBMCs of chronically HIV-1-infected HLA-B*52:01+ individuals were plated in 96-well polyvinylidene plates (Millipore, Bedford, MA) that had been precoated with 5 μg/ml anti-IFN-γ MAb 1-DIK (Mabtech, Stockholm, Sweden). The appropriate amount of each peptide (100 or 10 nM) was added in a volume of 50 μl, and then PBMCs were added at 1×10^5 cells/well in a volume of 100 μl. The plates were incubated for 40 h at 37°C in 5% CO$_2$ and then washed with phosphate-buffered saline (PBS) before the addition of biotinylated anti-IFN-γ MAb (Mabtech) at 1 μg/ml. After the plates had been incubated at room temperature for 100 min and then washed with PBS, they were incubated with streptavidin-conjugated alkaline phosphatase (Mabtech) for 40 min at room temperature. Individual cytokine-producing cells were detected as dark spots after a 20-min reaction with 5-bromo-4-chloro-3-indolylphosphate and nitroblue tetrazolium by using an alkaline phosphatase-conjugate substrate (Bio-Rad, Richmond, CA). The spots were counted by an Eliphoto-Counter (Minerva Teck, Tokyo, Japan). PBMCs without peptide stimulation were used as a negative control. Positive responses were defined as those greater than the mean of the negative-control wells plus 2 standard deviations (SD) (the number of spots in wells without peptides).

HIV-1 replication suppression assay. The ability of HIV-1-specific CTLs to suppress HIV-1 replication was examined as previously described (32). CD4+ T cells isolated from PBMCs derived from an HIV-1-seronegative individual with HLA-B*52:01, HLA-B*51:01, or both were cultured. After the cells had been incubated with the desired HIV-1 clones for 4 h at 37°C, they were washed three times with RPMI 1640-10% FCS medium. The HIV-1-infected CD4+ T cells were then cocultured with Pol283-8-specific CTL clones. From day 3 to day 7 postinfection, culture supernatants were collected and the concentration of p24 antigen (Ag) in them was measured by use of an enzyme-linked immunosorbent assay kit (HIV-1 p24 Ag ELISA kit; ZeptoMetrix).

HLA stabilization assay with RMA-S cells expressing HLA-B*52:01 or HLA-B*51:01. The peptide-binding activity of HLA-B*52:01 or HLA-B*51:01 was assessed by performing an HLA stabilization assay with RMA-S cells expressing HLA-B*52:01 (RMA-S-B*52:01) or HLA-B*51:01 (RMA-S-B*51:01) as described previously (33). Briefly, RMA-S-B*51:01 and RMA-S-B*52:01 cells were cultured at 26°C for 16 to 24 h. The cells (2×10^5) in 50 μl of RPMI 1640 supplemented with 5% FCS (RPMI–5% FCS) were incubated at 26°C for 3 h with 50 μl of a solution of peptides at 10^{-3} to 10^{-7} M and then at 37°C for 3 h. After having been washed with RPMI–5% FCS, the cells were incubated for 30 min on ice with an appropriate dilution of TP25.99 MAb. After two washings with RPMI–5% FCS, they were incubated for 30 min on ice with an appropriate dilution of fluorescein isothiocyanate (FITC)-conjugated anti-mouse Ig antibodies. Finally, the cells were washed three times with RPMI–5% FCS and the fluorescence intensity of the cells was measured by the FACS-Cant II. Relative mean fluorescence intensity (MFI) was calculated by subtracting the MFI of cells not peptide pulsed from that of the peptide-pulsed ones.

Sequencing of plasma RNA. Viral RNA was extracted from the plasma of chronically HIV-1-infected Japanese individuals by using a QIAamp

Mini Elute Virus spin kit (Qiagen). cDNA was synthesized from the RNA with Superscript II and random primer (Invitrogen). We amplified HIV RT and integrase sequences by nested PCR with RT-specific primers 5'-CCAAAAGTTAAGCAATGGCC-3' and 5'-CCCATCCAAAGGAATGG AGG-3' or 5'-CCTTGCCCCTGCTTCTGTAT-3' for the first-round PCR and 5'-AGTTAGGAATACCACACCCC-3' and 5'-GTAAATCCCC ACCTCAACAG-3' or 5'-AATCCCCACCTCAACAGAAG-3' for the second-round PCR and integrase-specific primers 5'-ATCTAGCTTTGCAG GATTCGGG-3' and 5'-CCTTAACCGTAGTACTGGTG-3' or 5'-CCTG ATCTCTTACCTGTCC-3' for the first-round PCR and 5'-AAAGGTCT ACCTGGCATGGG-3' or 5'-TTGGAGAGCAATGGCTAGTG-3' and 5'-AGTCTACTTGTCCATGCATGGC-3' for the second-round PCR. PCR products were sequenced directly or cloned with a TOPO TA cloning kit (Invitrogen) and then sequenced. Sequencing was done with a BigDye Terminator v1.1. cycle sequencing kit (Applied Biosystems) and analyzed by an ABI PRISM 310 Genetic Analyzer.

Statistical analysis with phylogenetically corrected odds ratios. Strength of selection was measured by using a phylogenetically corrected odds ratio as previously described (19). Briefly, the odds of observing a given amino acid (e.g., 135V) was modeled as $P/(1 - P) = (a \times X) + (b \times T)$, where P is the probability of observing 135V in a randomly selected individual, X is a binary (0/1) variable representing whether or not an individual expresses the HLA allele in question (e.g., B*52:01), and T equals 1 if the transmitted/founder virus for that individual carried 135V and -1 otherwise. Because the transmitted/founder virus is unknown, we averaged over all possibilities by using weights informed by a phylogeny that was constructed from the RT sequences of all of the individuals in the study. The parameters a and b were determined by using iterative maximum-likelihood methods. The maximum-likelihood estimate of a is an estimate of the natural logarithm of the odds ratio of observing 135V in individuals expressing X versus individuals not expressing X, conditioned on the individuals' (unobserved) transmitted/founder virus. P values are estimated by using a likelihood ratio test that compares the above model to a null model in which a equals 0.

To compare the odds of selection between two cohorts, we modified the phylogenetically corrected logistic regression model to include a cohort term, $Z = X \times Y$, where X is the HLA allele, and Y is a 0/1 variable that indicates cohort membership, yielding $P/(1 - P) = (a \times X) + (b \times T) + (c \times Z)$, as previously described (19, 34). A P value testing if the odds of escape are different in the two cohorts was estimated by using a likelihood ratio test that compared this model to a null model where c equals 0.

Generation of HLA class I tetramers. HLA class I-peptide tetrameric complexes (tetramer) were synthesized as described previously (31, 35). The Pol283-8 peptide was used for the refolding of HLA-B*51:01 or HLA-B*52:01 molecules. Phycoerythrin (PE)-labeled streptavidin (Molecular Probes) was used for generation of the tetramers.

Tetramer binding assay. HLA-B*51:01-restricted and HLA-B*52:01-restricted CTL clones were stained at 37°C for 30 min with PE-conjugated HLA-B*51:01-tetramer and HLA-B*52:01-tetramer, respectively, at concentrations of 5 to 1,000 nM. After two washes with RPMI 1640 medium supplemented with 10% FCS (RPMI 1640–10% FCS), the cells were stained with FITC-conjugated anti-CD8 MAb at 4°C for 30 min, followed by 7-amino-actinomycin D at room temperature for 10 min. After two more washes with RPMI 1640–10% FCS, the cells were analyzed by the FACS-Cant II flow cytometer. The tetramer concentration that yielded the half-maximal MFI (the EC_{50}) was calculated by probit analysis.

Crystallization, data collection, and structure determination. Soluble HLA-B*52:01 (with beta-2 microglobulin and peptide TAFTIPSI) was prepared as described above. Prior to crystallization trials, HLA-B*52:01 was concentrated to a final concentration of 20 mg ml^{-1} in 20 mM Tris-HCl (pH 8.0) buffer containing 250 mM NaCl. This was done with a Millipore centrifugal filter device (Amicon Ultra-4, 10-kDa cutoff; Millipore). Screening for crystallization was performed with commercially available polyethylene glycol (PEG)-based screening kits, PEGs and PEGs II suites (Qiagen). Thin needle crystals were observed from PEGs II suite

23 (0.2 M sodium acetate, 0.1 M HEPES [pH 7.5], and 20% PEG 3000). Several conditions were further screened by the hanging-drop method with 24-well VDX plates (Hampton Research) by mixing 1.5 μl protein solution and 1.5 μl reservoir to be equilibrated against reservoir solution (0.5 ml) at 293 K. Best crystals were grown from macro seeding with the initial crystals obtained with 0.2 M sodium acetate, 0.1 M Bis Tris propane [pH 7.5], and 20% PEG 3350.

The data set was collected at beamline BL41XU of SPring-8 with Rayonix charge-coupled device detector MX225HE. Prior to diffraction data collection, crystals were cryoprotected by transfer to a solution containing 25% (vol/vol) glycerol and incubation in it for a few seconds, followed by flash cooling. The data sets were integrated with XDS (36) and then merged and scaled by using Scala (37). HLA-B*52:01 crystals belonged to space group $P2_12_12_1$, with unit cell parameters $a = 69.0$ Å, $b = 83.3$ Å, and $c = 170.3$ Å. Based on the values of the Matthews coefficient (V_M) (38), we estimated that there were two protomers in the asymmetric unit with a V_M value of 1.37 Å^3/Da (Vsolv = 10.5%). For details of the data collection and processing statistics, see Table S1 in the supplemental material.

The structure was solved by the molecular replacement method with Molrep (39). The crystal structure of HLA-B*51:01 (PDB ID: 1E28) was used as a search model. Structure refinement was carried out by using Refmac5 (40) and phenix (41). The final model was refined to an Rfree factor of 34.7% and an R factor of 29.5% with a root mean square deviation of 0.014 Å in bond length and 1.48° in bond angle for all reflections between resolutions of 38.8 and 3.1 Å. Table S1 in the supplemental material also presents a summary of the statistics for structure refinement. The stereochemical properties of the structure were assessed by Procheck (42) and COOT (43) and showed no residues in the disallowed region of the Ramachandran plot.

Protein structure accession number. Atomic coordinates and structure factors for HLA-B*52:01 have been deposited in the Protein Data Bank under accession code 3W39.

RESULTS

Association of I135X variants with HLA-B*52:01. To clarify the possibility that CTLs restricted by other HLA alleles select the I135X mutation, we investigated the association between other HLA alleles and this mutation in 257 Japanese individuals chronically infected with HIV-1. We found an association of HLA-B*52:01 with the I135X variant, though this association was weaker than that with HLA-B*51:01 (phylogenetically corrected ln odds ratio [lnOR] of 11.76 [$P = 8.77 \times 10^{-4}$] for B*52:01 versus an lnOR of 40.0 [$P = 5.78 \times 10^{-12}$] for B*51:01; Table 1). We also analyzed the effects of HLA-B*52:01 and HLA-B*51:01 in chronically HIV-1-infected Japanese individuals, excluding HLA-B*51:01$^+$ and HLA-B*52:01$^+$ individuals, respectively, and found a significant association between HLA-B*52:01 and I135X variants among 200 HLA-B*51:01-negative individuals with chronic HIV-1 infection ($P = 4.7 \times 10^{-4}$; see Fig. S1A in the supplemental material) and that of HLA-B*51:01 with the variants in 202 HLA-B*52:01-negative ones ($P = 5.3 \times 10^{-8}$; see Fig. S1B in the supplemental material). These results together imply that HLA-B*52:01-restricted CTLs selected this mutation.

Identification of HLA-B*52:01-restricted, Pol283-specific CTLs. To identify the HLA-B*52:01-restricted HIV-1 epitope including RT135, we first investigated whether overlapping peptides covering RT135 could elicit CD8$^+$ T cells specific for these peptides in chronically HIV-1-infected individuals. We identified CTLs recognizing the Pol11-142 (TAFTIPSINNE) peptide in a chronically HIV-1-infected HLA-B*52:01$^+$ donor, KI-069 (see Materials and Methods). Since the C terminus of HLA-B*52:01-binding peptides is known to be a hydrophobic residue (30, 44), we speculated that TAFTIPSI (Pol283-8) was the epitope peptide.

TABLE 1 HLA-B*52:01 and HLA-B*51:01 association with variation at RT135 in Japanese and Caucasian cohorts

HLA class I allele	RT135 target variable	PlyloLOR[a]		Within-cohort P value		P value comparing cohorts
		Japanese	IHAC	Japanese	IHAC	
B*51:01	T	13.70	4.53	4.66×10^{-6}	1.70×10^{-35}	0.042
B*52:01	T	−9.77	1.25	0.464	2.04×10^{-3}	0.62
B*51:01	I	−40.00	−5.71	5.78×10^{-12}	1.58×10^{-51}	0.052
B*52:01	I	−11.76	−3.06	8.77×10^{-4}	2.95×10^{-5}	0.52
B*51:01	V	−9.76	8.52	0.884	0.41	0.85
B*52:01	V	12.21	10.15	0.076	1.82×10^{-3}	0.037
B*51:01	R	12.08	13.02	0.038	2.36×10^{-3}	0.42
B*52:01	R	0.26	8.37	0.423	0.469	0.89
B*51:01	L	−0.89	3.21	1	0.038	0.17
B*52:01	L	−0.56	3.61	1	0.231	0.29
B*51:01	K	−0.71	−40.00	1	0.53	0.99
B*52:01	K	−0.69	−40.00	1	0.779	0.99
B*51:01	M	7.76	12.00	0.894	2.10×10^{-4}	0.34
B*52:01	M	11.09	−40.00	0.034	0.517	0.12

[a] PlyloLOR, phylogenetically corrected lnOR.

Indeed, bulk-cultured T cells that had been cultured for 2 weeks after stimulation with Pol17-48 recognized C1R-B*52:01 cells prepulsed with Pol283-8 peptide at a much lower concentration than those incubated with the Pol11-142 peptide (Fig. 1A), strongly suggesting that Pol283-8 is an epitope recognized by HLA-B*52:01-restricted CTLs. These findings were confirmed by ELISPOT assay with PBMCs from two HLA-B*52:01[+] individuals

chronically infected with HIV-1 (Fig. 1B). To clarify whether this peptide was processed and presented by HLA-B*52:01, we investigated the killing activity of bulk-cultured T cells against HLA-B*52:01^{+} target cells infected with a vaccinia virus–HIV-1 Gag/Pol recombinant. They killed target cells infected with this recombinant but not those infected with wild-type vaccinia virus (Fig. 1C), indicating that the Pol283-8 peptide was presented by
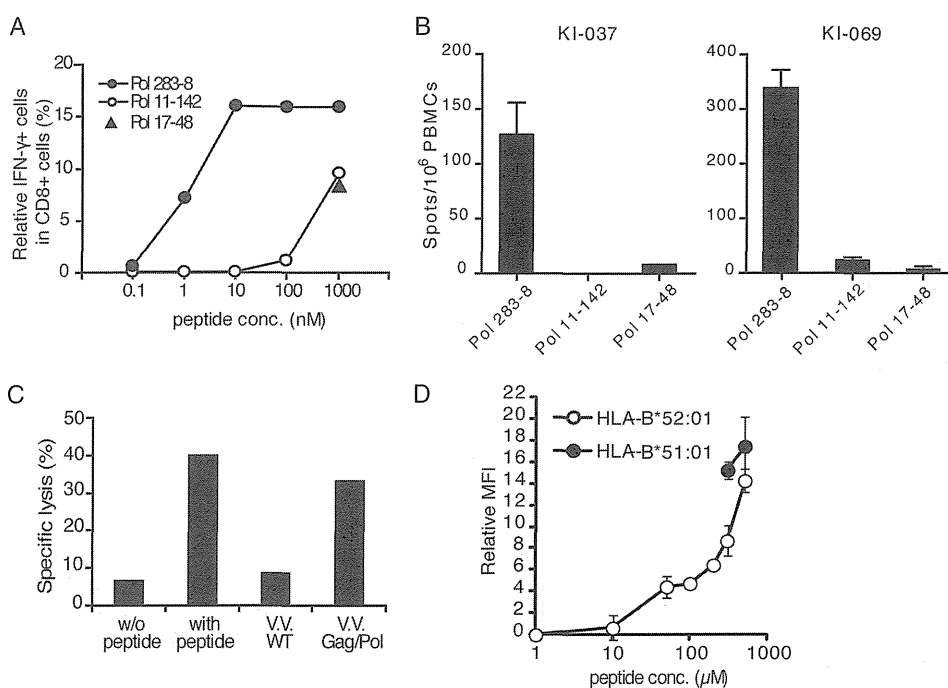

FIG 1 Identification of HLA-B*52:01-restricted Pol epitope. (A) Identification of the epitope peptide recognized by HLA-B*52:01-restricted CD8^{+} T cells. Bulk T cells were cultured for 2 weeks after stimulation with the Pol17-48 peptide, and then the recognition of C1R-HLA-B*52:01 cells prepulsed with Pol17-48, Pol11-142, or Pol283-8 peptide was assessed by ICS assay. (B) Pol283-8 peptide recognition by T cells ex vivo. Recognition of the Pol17-48, Pol11-142, or Pol283-8 peptide by PBMCs from two HLA-B*52:01[+] individuals chronically infected with HIV-1 (KI-037 and KI-069) was analyzed by ELISPOT assay. A 100 nM concentration of each peptide was used. (C) Killing activity of Pol283-specific, HLA-B*52:01-restricted CD8^{+} T cells against cells infected with a vaccinia virus–HIV-1 Gag/Pol recombinant. The killing activities of bulk-cultured T cells stimulated with Pol11-142 against target cells infected with a vaccinia virus–HIV-1 Gag/Pol recombinant (Gag/Pol) and against those infected with wild-type vaccinia virus (V.V. WT) are shown. (D) Binding of Pol283-8 peptide to HLA-B*52:01. Binding ability was measured by performing the HLA class I stabilization assay with RMA-S-B*52:01. RMA-S-B*51:01 cells were used as control cells for the Pol283-8 peptide.

TABLE 2 Pol283-8-specific CD8$^+$ T cells in chronically HIV-1-infected, HLA-B*52:01$^+$ individuals

Patient ID	HLA class I alleles		No. of CD4 cells/μl	No. of CD8 cells/μl	Viral load (no. of copies/ml)	Antiretroviral therapy	Relative IFN-γ$^+$/CD8$^+$ % in ICC assay	No. of spots/10^6 PBMCs in ELISPOT^a assay
KI-037	A*24:02/−	B*52:01/40:02	465	973	76,000	−	64.1	150
KI-090	A*24:02/−	B*52:01/55:01	606	511	≤50	+	40.2	80
KI-106	A*24:02/33:03	B*52:01/07:01	433	890	≤50	+	1.4	<79
KI-126	A*24:02/31:01	B*52:01/40:01	465	NT^b	36,000	−	60.4	<79
KI-130	A*24:02/−	B*52:01/07:02	351	1,275	14,000	−	0.0	<79
KI-167	A*24:02/−	B*52:01/54:01	455	909	26,000	−	0.0	<79
KI-067	A*24:02/−	B*52:01/48:01	234	1,198	89,000	−	10.9	<79
KI-071	A*24:02/31:01	B*52:01/40:06	292	1,134	48,000	−	0.7	<79
KI-076	A*02:01/24:01	B*52:01/40:01	136	252	14,000	−	61.0	80
KI-114	A*02:01/24:01	B*52:01/27:04	416	463	≤50	+	0.1	<79
KI-056	A*24:02/−	B*52:01/40:02	290	844	8,200	−	-0.1	<79
KI-108	A*24:02/−	B*52:01/−	373	481	NT	−	1.0	<79
KI-028	A*24:02/26:01	B*52:01/48:01	1,351	811	≤50	+	0.5	<79
KI-069	A*24:02/−	B*52:01/40:06	448	1,631	4,400	−	18.1	790

^{a} More than the mean number of negative-control spots + 2 SD was defined as a positive response (positive response, >79 spots).
^{b} NT, not tested.

HLA-B*52:01. We analyzed the binding of the Pol283-8 peptide to HLA-B*52:01 by using the HLA stabilization assay. The results demonstrated that this peptide bound to HLA-B*52:01 (Fig. 1D). These results together indicate that the Pol283-8 epitope can therefore be presented by both HLA-B*51:01 and HLA-B*52:01.

We investigated whether Pol283-8-specific CD8$^+$ T cells were elicited predominantly in chronically HIV-1-infected HLA-B*52:01$^+$ HLA-B*51:01$^−$ individuals. PBMCs from 14 of these individuals were analyzed by ICS assay with Pol283-8 peptide-stimulated culture cells, as well as by ELISPOT assay. The results of the ICS assay showed that 7 of these 14 HLA-B*52:01$^+$ HLA-B*51:01$^−$ patients had Pol283-specific CD8$^+$ T cells, whereas those of the ELISPOT assay with *ex vivo* PBMCs revealed that Pol283-specific CD8$^+$ T cells were detected in only four individuals (Table 2). These results suggest that the three individuals in whom the specific CTLs were detected by the ICS assay but not by the ELISPOT assay may have memory T cells. These results together indicate that Pol283-8 was recognized as an HLA-B*52:01-restricted immunodominant epitope in the HLA-B*52:01$^+$ individuals and support the idea that the I135X mutation was selected by HLA-B*52:01-restricted, Pol283-8-specific CD8$^+$ T cells.

Strong ability of HLA-B*52:01-restricted, Pol283-8-specific CD8$^+$ T cells to suppress HIV-1 replication. A previous study showed that HLA-B*51:01-restricted, Pol283-8-specific T cells have a strong ability to kill HIV-1-infected target cells and to suppress HIV-1 replication (31). Therefore, we expected that the HLA-B*52:01-restricted T cells also would have this strong ability. We generated HLA-B*52:01-restricted, Pol283-8-specific T cell clones and investigated their ability to kill peptide-pulsed or HIV-1-infected target cells. Clone 1E1 effectively killed C1R-B*52:01 cells prepulsed with the Pol283-8 peptide (Fig. 2A) and NL-432-infected CD4$^+$ T cells from an HLA-B*52:01$^+$ individual (Fig. 2B). Additional T cell clones also showed strong killing activity against NL-432-infected HLA-B*52:01$^+$ CD4$^+$ T cells (data not shown). In addition, we investigated the ability of these CTL clones to suppress HIV-1 replication. CD4$^+$ T cells derived from an HLA-B*52:01$^+$ individual were infected with NL-432 or M20A mutant virus, the latter of which has an amino acid substitution at position 20 of Nef and lacks the ability to downregulate the surface

expression of HLA-A and -B molecules (Fig. 2C). Representative data on the 1E1 clone and summary data on four clones are shown in Fig. 2D and E, respectively. These CTL clones strongly suppressed the replication of both the NL432 and M20A mutant viruses, indicating that the HLA-B*52:01-restricted CTLs had a strong ability to suppress HIV-1 replication, as was the case with the HLA-B*51:01-restricted ones.

Recognition of I135X mutations by Pol283-8-specific, HLA-B*52:01-restricted CTLs. Four mutations (8T, 8L, 8R, and 8V) were observed predominantly at RT135 in chronically HIV-1-infected HLA-B*52:01$^+$ individuals (Fig. 3). These mutations may have been selected by Pol283-8-specific, HLA-B*52:01-restricted CTLs in these patients. We therefore investigated the ability of HLA-B*52:01-restricted CTLs to suppress the replication of these mutant viruses *in vitro*. The CTL clones failed to suppress the replication of the 8L, 8T, or 8R mutant, though they weakly suppressed that of the 8V virus at an E/T cell ratio of 1:1 (Fig. 4A). These results support the idea that these variants were escape mutations from the HLA-B*52:01-restricted CTLs. To clarify the mechanism by which the CTL clones failed to suppress the replication of these mutant viruses, we investigated the CTL clones for recognition of C1R-B*52:01 cells prepulsed with the mutant peptides. The CTL clones effectively recognized the 8V peptide at the same level as the wild-type peptide and the 8T and 8L peptides at less than that of the wild-type one, whereas they failed to recognize the 8R peptide (Fig. 4B). An ELISPOT assay with *ex vivo* PBMCs from KI-069 showed that Pol283-8-specific CTLs effectively recognized the 8I and 8V variants but not the other three mutant peptides (Fig. 4C), suggesting that Pol283-8-specific CTLs failed to recognize the 8T, 8L, and 8R peptides *in vivo*. The lack of recognition of these mutants by CTLs may be attributable to a failure of T cell receptor (TCR) recognition, the inability of the peptide to bind to HLA-B*52:01, and/or disruption of the processing of the epitope in HIV-1-infected cells.

Different pattern of RT135 mutation selection by two HLA alleles. As described above, HLA-B*51:01 and HLA-B*52:01 were associated with I135X in a Japanese population in which the prevalence of HLA-B*51:01 and B*52:01 alleles is relatively high (21.9 and 21.1%, respectively). In a Japanese cohort, out of the five
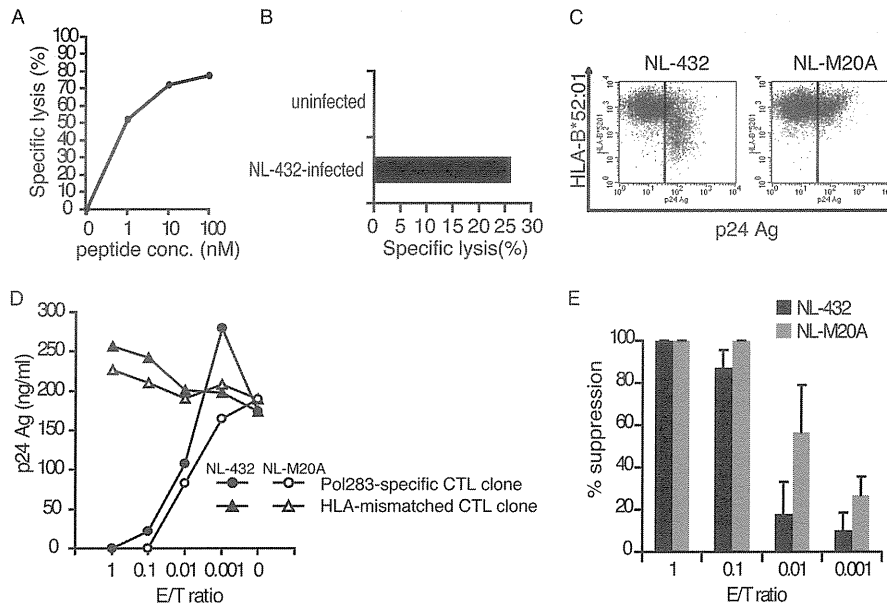
FIG 2 Abilities of HLA-B*52:01-restricted, Pol283-8-specific CD8$^+$ T cell clones to kill HIV-1-infected CD4$^+$ T cells and to suppress HIV-1 replication. (A) Killing activity of an HLA-B*52:01-restricted, Pol283-8-specific CD8$^+$ T cell clone against C1R-B*52:01 cells prepulsed with Pol283-8 peptides. The activity of an HLA-B*52:01-restricted, Pol283-8-specific CD8$^+$ T clone, 1E1, to kill C1R-B*52:01 cells was measured by performing a ^{51}Cr-release assay. (B) Killing activity of HLA-B*52:01-restricted, Pol283-8-specific CD8$^+$ T cell clone 1E1 against CD4$^+$ T cells infected with HIV-1. The ability of the clone to kill CD4$^+$ T cells infected with NL-432 was measured by performing a ^{51}Cr-release assay. (C) Downregulation of HLA-B*52:01 in HIV-1-infected CD4$^+$ T cells. CD4$^+$ T cells derived from an HLA-B*52:01$^+$ donor (HLA-A*11:01/A*24:02, HLA-B*52:01/B*52:01, and HLA-C*12:02/C*14:02) were infected with NL-432 and then cultured for 4 days. The cultured CD4$^+$ T cells were stained with anti-p24 Ag and TÜ109 anti-Bw4 MAbs. (D) Ability of an HLA-B*52:01-restricted, Pol283-8-specific CD8$^+$ T cell clone to suppress the replication of NL-432 and M20A mutant viruses. Suppressing ability was measured at four different E/T cell ratios (1:1, 0.1:1, 0.01:1, and 0.001:1). HIV-1-infected HLA-B*52:01$^+$ CD4$^+$ T cells were cocultured with an HLA-B*52:01-restricted, Pol283-8-specific CTL clone or an HLA-mismatched CTL clone at various E/T cell ratios. HIV-1 p24 Ag levels in the supernatant were measured on day 6 postinfection. (E) Summary of the ability of HLA-B*52:01-restricted, Pol283-8-specific CD8$^+$ T cell clones ($n = 4$) to suppress the replication of Nl-432 and M20A mutant viruses at four different E/T cell ratios.

amino acid mutations that can be generated by a one-nucleotide mutation from Ile, the T mutation was strongly associated with the presence of HLA-B*51:01 ($P = 4.66 \times 10^{-6}$), whereas HLA-B*52:01 was associated not with any single amino acid substitu-
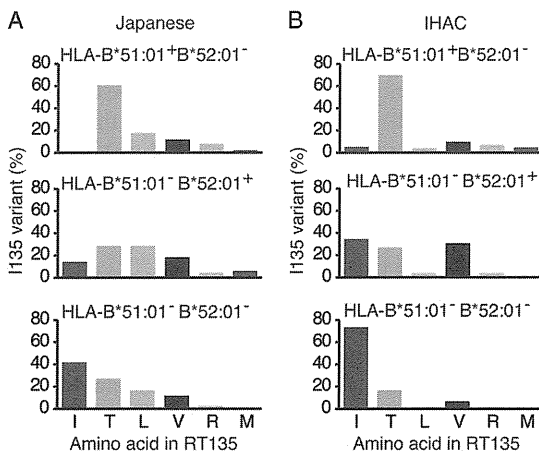

FIG 3 Amino acid variation at RT135 in Japanese individuals. (A) Frequency of the amino acid at RT135 in 51 HLA-B*51:01$^+$ HLA-B*52:01$^-$, 49 HLA-B*51:01$^-$ HLA-B*52:01$^+$, and 151 HLA-B*51:01$^-$ HLA-B*52:01$^-$ Japanese subjects. (B) Frequency of the amino acid at RT135 in 131 HLA-B*51:01$^+$ HLA-B*52:01$^-$, 26 HLA-B*51:01$^-$ HLA-B*52:01$^+$, and 1195 HLA-B*51:01$^-$ HLA-B*52:01$^-$ subjects in three predominantly Caucasian cohorts from Canada, the United States, and Western Australia (IHAC).
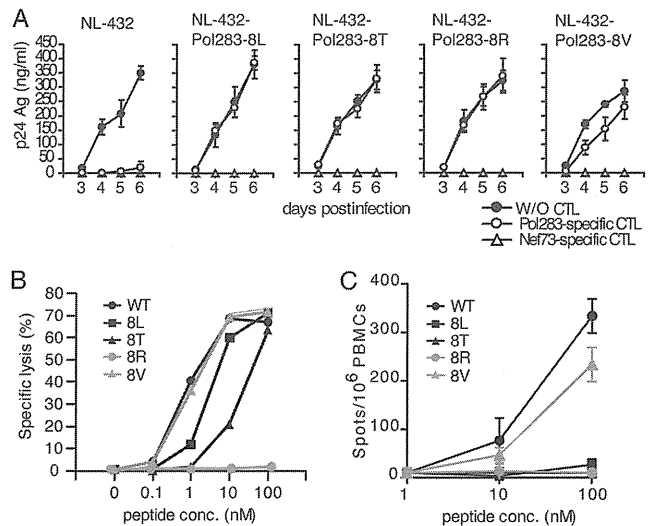

FIG 4 Ability of HLA-B*52:01-restricted, Pol283-8-specific CD8$^+$ T cell clones to suppress the replication of four mutant viruses. (A) Ability of an HLA-B*52:01-restricted, Pol283-8-specific CD8$^+$ T cell clone to suppress the replication of four (8L, 8T, 8R, and 8V) mutant viruses and NL-432. The abilities of an HLA-B*52:01-restricted, Pol283-8-specific CD8$^+$ T cell clone and an HLA-A*1101-restricted Nef73-specific T cell clone to suppress the replication of these viruses were measured at an E/T cell ratio of 1:1 on days 3 to 6. W/O, without. (B) Recognition by an HLA-B*52:01-restricted, Pol283-8-specific CD8$^+$ T cell clone of C1R-B*52:01 cells prepulsed with any one of the four mutant epitope peptides or the wild-type (WT) peptide (8I). (C) Recognition of mutant epitope peptides by ex vivo Pol283-8-specific CTLs. The recognition of the Pol283-8 peptide (WT) or the mutant epitope peptide by PBMCs from KI-069 was analyzed by ELISPOT assay.

440

tion but only with the non-I mutation ($P = 8.77 \times 10^{-4}$, Table 1). The distribution of amino acid variations at RT135 in the HLA-B*51:01$^+$ HLA-B*52:01$^-$ Japanese subjects was different from that in the HLA-B*51:01$^-$ HLA-B*52:01$^+$ ones (Fig. 3). These results suggest that the HLA-B*51:01-restricted CTLs strongly selected the 135T mutation but that the HLA-B*52:01-restricted ones selected a variety of different amino acids at this position in Japanese individuals.

We also analyzed the association of I135X mutations with HLA-B*52:01 and HLA-B*51:01 in three predominantly Caucasian cohorts from Canada, the United States, and Western Australia (International HIV Adaptation Collaborative [IHAC]) (19) comprising >1,200 subjects (Table 1). HLA-B*51:01 was very strongly associated with the I135X mutation (lnOR of 5.71; $P = 1.58 \times 10^{-51}$). Although only 2.1% of the IHAC cohort subjects expressed HLA-B*52:01, this allele was also associated with I135X (lnOR of 3.06; $P = 2.95 \times 10^{-5}$). The T mutation was strongly associated with HLA-B*51:01 ($P = 1.70 \times 10^{-35}$), whereas the T and V mutations were weakly associated with HLA-B*52:01 ($0.0005 < P < 0.005$). Thus, these results showed a similar selection of RT135 mutations by HLA-B*52:01 in the predominantly Caucasian cohort, despite a substantially lower frequency of HLA-B*52:01. The magnitude of the strength of selection by HLA-B*52:01 and HLA-B*51:01 on RT135 did not differ significantly between the two cohorts (Table 1). These results indicate that HLA-B*51:01 strongly selected 135T but that HLA-B*52:01 selected a variety of substitutions at this site (designated I135X) in both the Japanese and non-Japanese cohorts.

Comparison of TCR affinity and abilities of HLA-B*51:01-restricted and HLA-B*52:01-restricted CTLs to suppress HIV-1 replication. We investigated the TCR affinity of HLA-B*51:01-restricted and HLA-B*52:01-restricted CTL clones by using tetramers of the HLA-B*51:01-Pol283 peptide and the HLA-B*52:01-Pol283 peptide complex (HLA-B*51:01 and HLA-B*52:01 tetramers, respectively). The TCR affinity of these CTL clones was compared in terms of EC_{50}. The EC_{50} of the HLA-B*51:01-restricted CTL clones was significantly lower than that of the HLA-B*52:01-restricted CTL clones (Fig. 5A), suggesting that the former CTL clones had TCRs with a higher affinity for the ligand than those of the latter clones. These results imply that the HLA-B*51:01-restricted CTL clones could recognize the HIV-1-infected targets more effectively than HLA-B*52:01-restricted ones.

Since CD4$^+$ T cells derived from an HLA-B*52:01 homozygous individual were used in the experiment shown in Fig. 2D and E, the ability of the HLA-B*52:01-restricted CTL clones to suppress the replication of NL-432 may have been overestimated. To evaluate and compare the abilities of HLA-B*51:01-restricted and HLA-B*52:01-restricted CTL clones to suppress the replication of NL-432, we used CD4$^+$ T cells from individuals expressing HLA-B*51:01$^+$/B*52:01$^-$, HLA-B*51:01$^-$/B*52:01$^+$, or HLA-B*51:01$^+$/B*52:01$^+$ (Fig. 5B). Two HLA-B*51:01-restricted CTL clones strongly inhibited the replication of HIV-1 in cultures of NL-432-infected HLA-B*51:01$^+$/B*52:01$^-$ CD4$^+$ T cells but not in those of HLA-B*51:01$^-$/B*52:01$^+$ cells, whereas two HLA-B*52:01-restricted CTL clones strongly inhibited the replication of HIV-1 in cultures of NL-432-infected HLA-B*51:01$^-$/B*52:01$^+$ CD4$^+$ T cells but not in those of HLA-B*51:01$^+$/B*52:01$^-$ cells (Fig. 5B, left and middle). The ability of the HLA-B*51:01-restricted CTL clones to suppress the replication of HIV-1 was greater than that of the HLA-B*52:01-restricted CTL clones. This was confirmed by
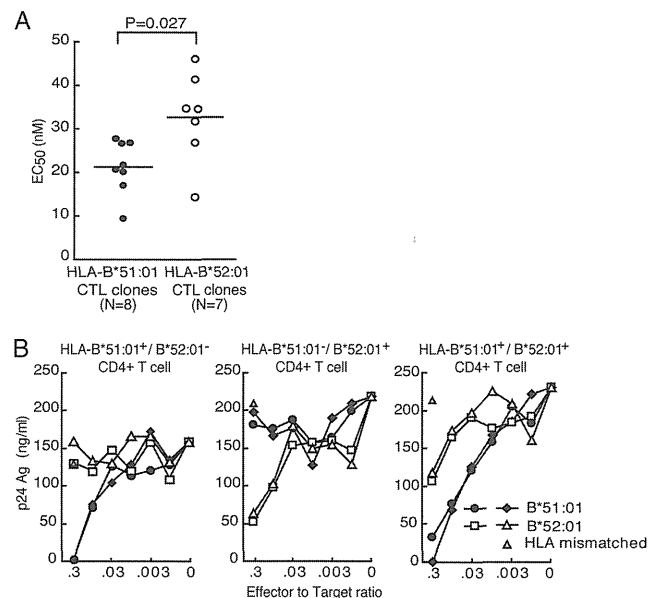

FIG 5 Differences between HLA-B*51:01-restricted and HLA-B*52:01-restricted CD8$^+$ T cell clones in TCR avidity and the ability to suppress HIV-1 replication. (A) TCR avidity of the HLA-B*51:01-restricted and HLA-B*52:01-restricted CTL clones expressed as EC_{50}. The ability of the TCRs of HLA-B*51:01-restricted and HLA-B*52:01-restricted CTL clones to bind HLA-B*51:01 tetramers and HLA-B*52:01 tetramers, respectively, was measured in terms of the MFI of each CTL clone stained with the tetramers at concentrations of 5 to 1,000 nM. (B) The ability of two HLA-B*51:01-restricted and two HLA-B*52:01-restricted CD8$^+$ T cell clones to suppress HIV-1 was measured at six different E/T cell ratios (0.3:1, 0.1:1, 0.03:1, 0.01:1, 0.003:1, and 0.001:1). CD4$^+$ T cells from individuals expressing HLA-B*51:01$^+$/B*52:01$^-$, HLA-B*51:01$^-$/B*52:01$^+$, or HLA-B*51:01$^+$/B*52:01$^+$ were infected with NL-432 and then cocultured with a given Pol283-8-specific CTL clone or an HLA-mismatched CTL clone. HIV-1 p24 Ag levels in the supernatant were measured on day 5 postinfection.

the experiment with HLA-B*51:01$^+$/B*52:01$^+$ CD4$^+$ T cells (Fig. 5B, right). Although both HLA-B*51:01-restricted and HLA-B*52:01-restricted CTL clones strongly inhibited the replication of HIV-1 in the cultures of NL-432-infected HLA-B*51:01$^+$/B*52:01$^+$ CD4$^+$ T cells, the former clones exhibited a greater ability to suppress the replication of HIV-1 than did the latter cells. These results indicate that the HLA-B*51:01-restricted CTL clones had a stronger ability to suppress HIV-1 replication than the HLA-B*52:01-restricted clones. Taken together, both our *in vitro* and our *in vivo* (population level HLA-association) data suggest that immune pressure on RT135 by HLA-B*51:01-restricted T cells was stronger than that imposed by HLA-B*52:01-restricted cells.

Structural basis of the difference in recognition between HLA-B*52:01- and HLA-B*51:01-restricted CTLs. In order to investigate the structural basis of the difference in recognition between HLA-B*52:01- and HLA-B*51:01-restricted CTLs, we performed a crystallographic study of the HLA-B*52:01 molecule complexed with the Pol283-8 peptide. The recombinant HLA-B*52:01 protein was crystallized, and by using the molecular replacement method, the three-dimensional structure of HLA-B*52:01 complexed with the Pol283-8 peptide was successfully determined. The crystal and statistical data are summarized in Table S1 in the supplemental material. The overall structure and peptide-binding mode were similar to those of HLA-B*51:01 complexed with the same Pol283-8 peptide (Fig. 6A and B), which
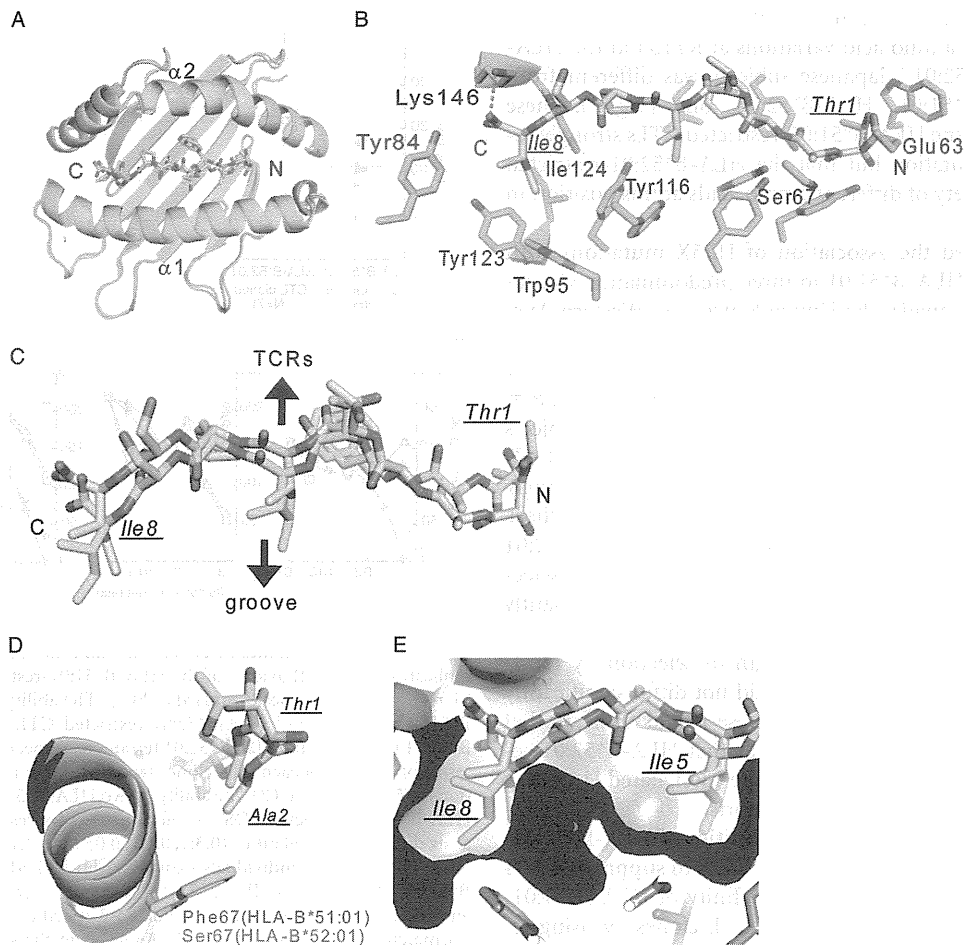
441

FIG 6 Structural comparison of HLA-B*52:01 and HLA-B*51:01 molecules complexed with the Pol283-8 peptide. (A) Crystal structures of HLA α1-α2 domains complexed with the Pol283-8 peptide (stick model) on the HLA-B*52:01 (green, yellow) and HLA-B*51:01 (cyan, cyan) complexes. This same coloring also applies to panels B to E. (B) Pol283-8 peptide and interacting side chains on the HLA-B*52:01 complex. Hydrogen bonds are shown as blue dotted lines. (C) Comparison of the Pol283-8 peptide conformations of HLA-B*52:01 and HLA-B*51:01 complexes. (D) N-terminal side of HLA-B*52:01 and HLA-B*51:01 complexes. (E) C-terminal side of HLA-B*52:01 and HLA-B*51:01 complexes. Surface presentation for the α1-α2 domains is shown in gray.

we had previously reported (45). This finding explains the cross presentation of this peptide by both HLA alleles. On the other hand, there was a notable conformational difference in the N-terminal region of the peptide between the two alleles (Fig. 6C and D). The replacement of Phe67 of HLA-B*51:01 with Ser in HLA-B*52:01 makes a local space, causing the N-terminal region of the peptide (T1 and A2) to reside deeper in the peptide-binding groove. Furthermore, the Gln63Glu mutation in HLA-B*52:01 affords a new interaction with the T1 residue of the peptide. These changes would, to some extent, have hidden the side chains of T1 and A2 (flat surface) from the TCRs, which may have reduced their interactions with TCRs on the HLA-B*52:01-restricted CTLs. On the other hand, the conformation of the C-terminal region of the peptide complexed with HLA-B*51:01 or HLA-B*52:01 was similar, even though C-terminal Ile8 of the peptide exhibited shallower penetration of the hydrophobic groove in the case of HLA-B*52:01 than in that of HLA-B*51:01 (Fig. 6C and E). These results may indicate that the relatively flat surface of the N-terminal side of the peptide contributed to the lower affinity for TCRs in the case of HLA-B*52:01.

DISCUSSION

HLA-B*52:01 and HLA-B*51:01 differ by only two residues, at positions 63 and 67 (44). Substitutions at these residues affect the formation of the B pocket in the peptide-binding pocket (45), suggesting the possibility that HLA-B*52:01 has a peptide motif different from that of HLA-B*51:01. Indeed, HLA-B*52:01-binding peptides have P2 primary anchors that are different from HLA-B*51:01-binding ones (30, 46). Since the Pol283-8 epitope carries Ala at its second position and Ile at the C terminus of the peptide, it is likely that this peptide would effectively bind to HLA-B*51:01 but not to HLA-B*52:01. However, the results of the HLA stabilization assay demonstrated that the Pol283-8 peptide did effectively bind to HLA-B*52:01. Since the HLA-B*52:01-binding peptide is known to have Pro as its preferred P2 anchor residue, this peptide carrying Ala at position 2 may be capable of binding to HLA-B*52:01. A previous study showed cross-recognition of alloreactive T cells between HLA-B*51:01 and HLA-B*52:01 (47, 48), indicating that some self-peptides can be presented by both of these HLA class I molecules. The findings on the crystal structure

442